4.8 Results of Laboratory Work

For consideration and understanding the geological features of the geological survey microscopic observations, X-ray diffraction analysis and chemical analysis were conducted for the rock samples collected during the geological mapping. All the samples used for laboratory work were collected from the outcrop described during the geological mapping.

4.8.1 Observation of Thin Sections of Rock Samples and Polished Sections of Ore Samples

During the geological survey of the Attapeu Area, producing 1:200,000 scale geological map, rock samples and ore samples were collected from the outcrop to make thin sections and polished sections for detail consideration of the area. The thin sections and polished section were made in DGEO together with counterparts as a part of technical training.

1) Observation of Thin Sections

A total of 52 thin sections were made for the typical samples representing each rock facies and altered rock. The results of microscopic observation were given in Annex 5.

2) Observations of Polished Sections

A total of 8 thin sections were made for the ore samples collected from mineral showings found in the Attapeu Area. The results of microscopic observation are given in Annex 6. Pyrite and hematite are only ore minerals found by the microscopic observation.

4.8.2 X-ray Diffraction Analysis

The x-ray diffraction analysis was conducted for the samples collected during geological survey (1,200,000 scale geological map) of the second and third surveys. Igneous rocks and sedimentary rocks were selected for the x-ray diffraction analysis.

The purpose of the x-ray diffraction analysis is to identify the secondary minerals produced by the hydrothermal alteration, weathering and diagenesis in the igneous rocks and sedimentary rock, and to characterize alteration of the area.

1) Analyzed Samples

X-ray diffraction analysis was conducted for 58 samples collected during the second and third surveys.

2) Analytical Method

The X-ray diffraction analysis was conducted at Dowa Techno Research Co., Japan, using Geiger Flex RAD-2C of Rigakudenki, Japan.

3) Results of X-ray diffraction Analysis

The results of X-ray diffraction analysis is given in Annex 7.

The mineral assemblages of quartz –sericite-chlorite, characterized by hydrothermal alteration, was found in most of the samples and in some of the samples pyrite was found in addition to them. It is an alteration characterized by sericite and is common alteration normally associated with epithermal mineralization of Au-Ag. The assemblage of alteration minerals suggests that hydrothermal solution responsible for this alteration is neutral to alkalic. Hematite and goethite found in some of the samples suggest oxidation during weathering. Talc was found in samples C011, C028a, C028b, C028c, C028d and C028e. This was produced by hydrothermal alteration of basalt (partly serpentinite) and these samples were collected near the gold mine of army concession. This suggests relatively strong hydrothermal alteration took place in the area.

4.8.3 Chemical Analysis of Igneous Rocks

Chemical analyses of the igneous rocks were conducted for granitic rock and basalt collected during the geological survey (1:200,000 scale) in the second and third surveys.

Although many types of igneous rocks occur in the Attapeu, granitic rocks and basalts are predominantly occur and these are classified into few lithological units. The purposes of the chemical analysis of the igneous rocks were conducted to characterize, geochemically, the igneous rock distributed in the area and to consider the tectonic setting in which these igneous rock were generated.

1) Analyzed samples

As shown in Annex 9, chemical analyses of 20 samples were conducted.

2) Contents of Chemical Analyses

Chemical analyses were conducted for 32 elements, including major elements, trace elements and rare earth elements (REE) as given below.

SiO_2, TiO_2, Al_2O_3, Fe_2O_3, MgO, MnO, CaO, Na_2O, K_2O, P_2O_5, LOI, Rb, Sr, Ba, Zr, V, Nb, Y, REE (La, Ce, Pr, Nd, Sm, Eu, Gd, Tb, Dy, Ho, Er, Tm, Yb, Lu)

3) Analytical Methods

Chemical analyses of all the elements except LOI (Loss of Ignition) were conducted by Inductively Coupled Plasma Mass Spectrometry (ICPMS) at ALS Chemex, Australia. LOI was determined gravimetrically after fusion in electric fumace.

4) Results of Chemical analyses

The analytical results are given in Annex 9. For understanding the geochemical nature of granitic and basaltic rocks, the results of chemical analyses were plotted on various petrochemical discrimination diagrams (Figures 4.8.1 to 4.8.15).

Based on the results of chemical analysis, geochemical characteristics of the granitic rocks are summarized as below.

a. All of the granite bodies fall in the areas of sub-alkali and calc-alkali field in the alkali-silica and FeO-alkali-MgO (AFM) diagram.

b. In the diagram of trace elements normalized to MORB (Figure 4.8.3), among the granite bodies, there are some differences in Ba , P, and Ti concentration and they are classified into 5 types.

- Hornblende-Biotite Granodiorite, distributed along Route 18B and in the area Xe Kaman River
- Biotite Granite – Granodiorite, distributed in the area Xe Kaman River
- Biotite-Hornblende- Quartz diorite, distributed in the area of Xe Kaman River
- Biotite-Hornblende Granodiorite, distributed in the area of Xe Xou River
- Biotite-Muscovite Granite, distributed in the area of Xe Xou River

c. In chondrite normalized pattern of REE diagram (Figure 4.8.4), the granitic rocks are separated in 4 groups given below by differences in concentrations of light REE, heavy REE and Eu.

- Hornblende-biotite granodiorite and biotite-hornblende-quartz diorite, distributed along the Route 18B and in the area of Xe Kaman River
- Biotite granite— granodiorite, distributed in the area of Xe Kaman River
- Biotite- hornblende granodiotite, distributed in the area of Xe Xou River
- Biotite-muscovite granite, distributed in the area of Xe Kaman River

Particularly, the biotite granite－granodiorite of the Xe Kaman River area is more enriched in heavy REE with larger Eu anomaly compared with granitic rocks of other bodies.

d. The most of the granitic rocks occupy the field of VAG (Volcanic Arc Granite) in Nb-Y, Rb-(Y+Nb) diagrams of tectonic setting of granite (Figure 4.8.5). The biotite granite－granodiorite, on the other hand, have higher Nb and Y concentrations compared with other granite bodies and they are plotted in the field of WPG (Within plate granite).

e. The granitic rocks of the area are separated in three groups by the Al_2O_3-CaO-alkali discrimination diagram of granitic rocks. They area:

- Meta-aluminous I-type granite: hornblende-biotite granodiorite and biotite-hornblende quartz diorite distributed along Route 18B and in the area of Xe Kaman River, biotite-hornblende granodiorite distributed in the area of Xe Xou River
- Per-aluminous S-Type granite: biotite-muscovite granite distributed in the area of Xe Xou River
- Meta-aluminous－per-alkaline I-A Type granite: biotite granite－granodiorite distributed in the area of the Xe Kaman River

f. The (Sr/Y)-Y discrimination diagram of tectonics for calc-alkali rocks shows that the granitic rocks of the area have different Y concentration depending on the each body. Biotite-hornblende granodiorite and biotite-muscovite granite distributed in the area of Xe-Xou River are ploted in the field of adakite.

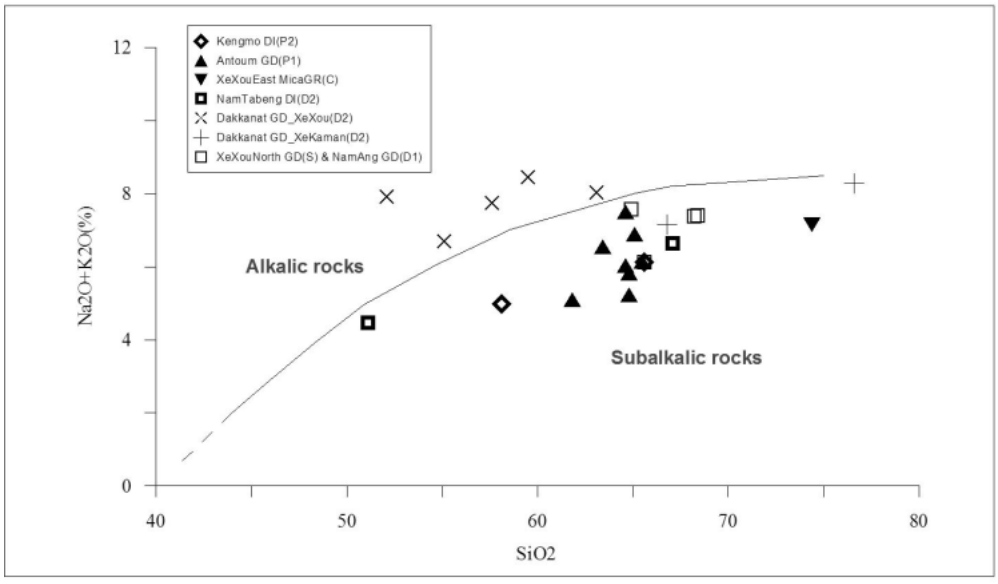

Figure 4.8.1 Alkali-silica diagram of the plutonic rocks

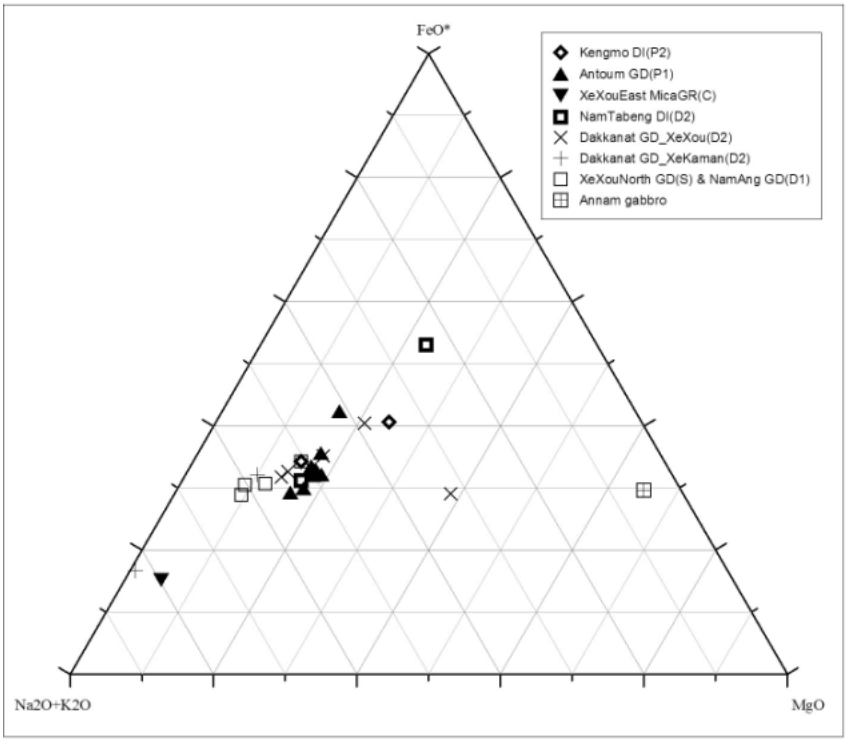

Figure 4.8.2 AFM diagram of the plutonic rocks

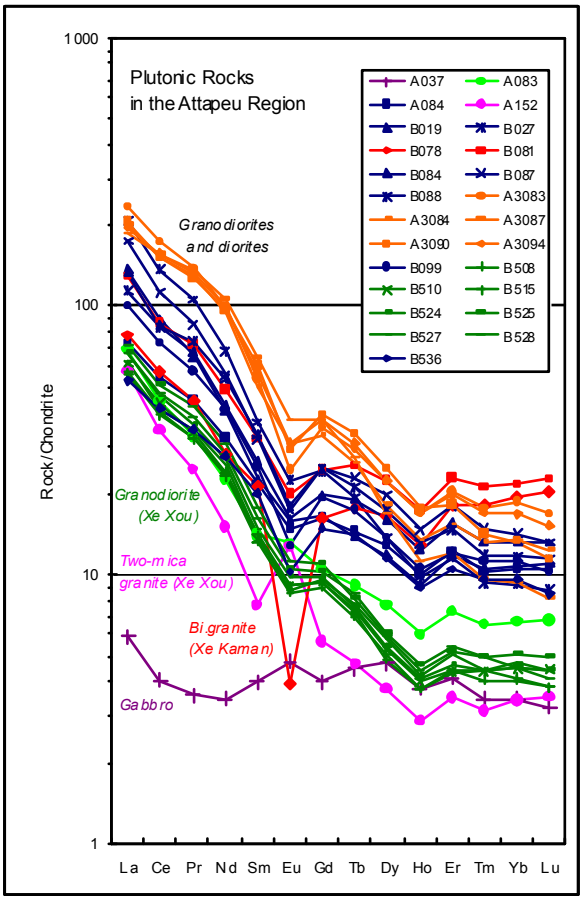

Figure 4.8.3 MORB normalized spider diagram of the plutonic rocks

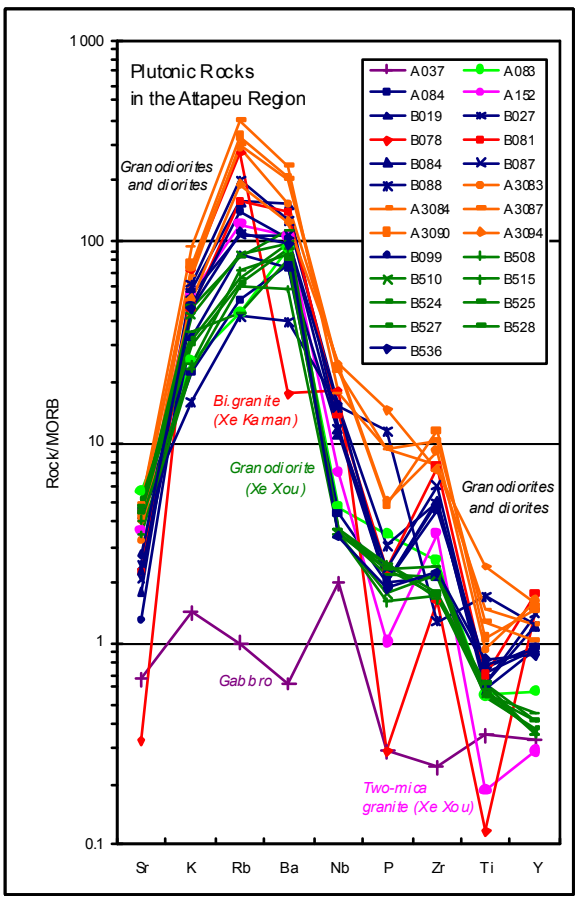

Figure 4.8.4 Chondrite normalized geochemical patterns of the plutonic rocks

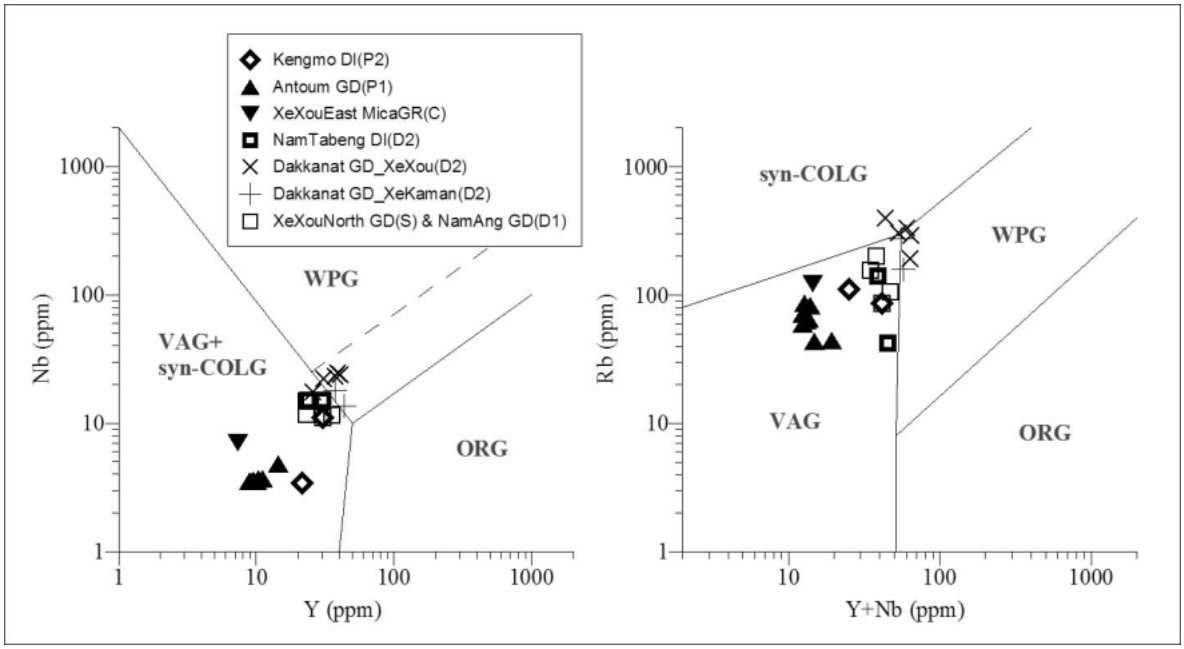

Figure 4.8.5 Discrimination of granitic rocks by trace elements

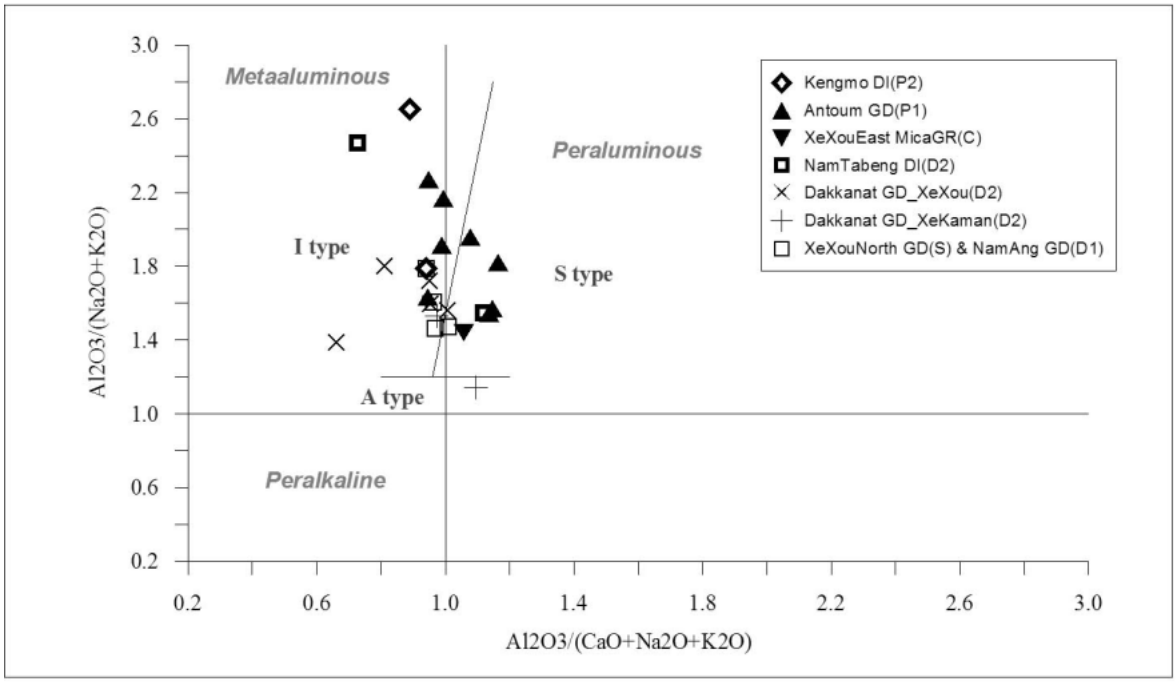

Figure 4.8.6 Discrimination diagram of granitic rocks by Al_2O_3 index

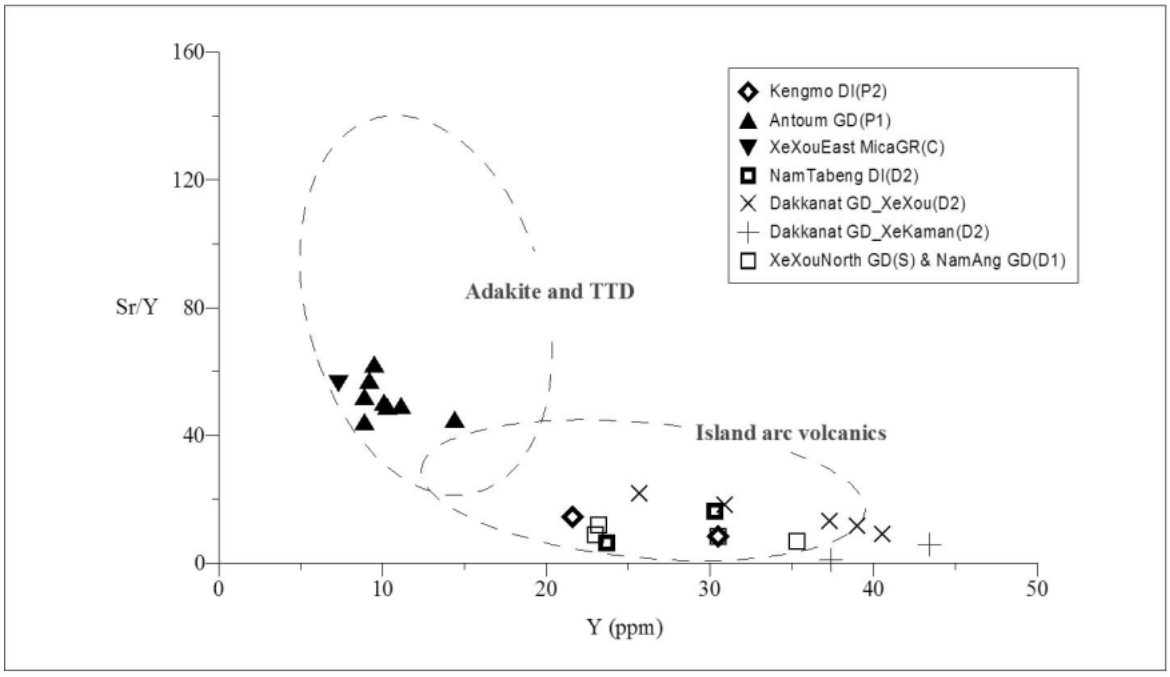

Figure 4.8.7 (Sr/Y)-(Y) discrimination diagram of granitic rock

Geochemical characteristics of the basaltic rocks are summarized below.

a. The alkali-silica diagrams (Figures 4.8.8 and 4.8.9) show that most of the samples are sub-alkalic basalt to basaltic andesite and only basalt samples of Bolavene Plateau (A005) is alkalic trachy basalt.

b. In FeO-alkali-MgO (AFM) (Figure 4.8.10) diagram of discriminating igneous trend , all of the samples are plotted in the similar field and no clear trend of differentiation is identified.

c. All the samples show similar patterns in the spider diagram of trace elements normalized to MORB (Figure 4.8.11) except basalt sample of Bolavene Plateau (A005) which is more enriched to trace elements than other samples.

d. Similar chondrite normalized patterns of REE with a slight variation of light REE concentration were obtained from the samples of basaltic rocks in the area (Figure 4.8.12). The light REE is slightly enriched in the basalt of the Bolavene Plateau (A005), while it is less in the basalt of the Xe Kong River area (B024).

e. In the (Ti/100))-Zr-3Y discrimination diagram of the tectonic setting of basalt generation (Figure 4.8.13), all samples fall in the field of WPB (within plate basalt).

f. All the basaltic rock samples are plotted in the fields of either WPA (within plate alkali) or WPI (within plate tholeiite) of the WPB (within plate basalt) in the 2Nb-(Zr//4)-Y discrimination diagram of tectonic setting (Figure 4.8.14).

g. In the TiO2-10MnO-10P2O5 discrimination diagram for basaltic rocks (Figure 4.8.15), most of the samples of basaltic rocks occupy the filed of OIA (oceanic-island alkali basalt or seamount alkali basalt) except one taken in the area of the Xe Kong River (B024) which is plotted in the field of OIT (oceanic-island tholeiite of seamount tholeiite)

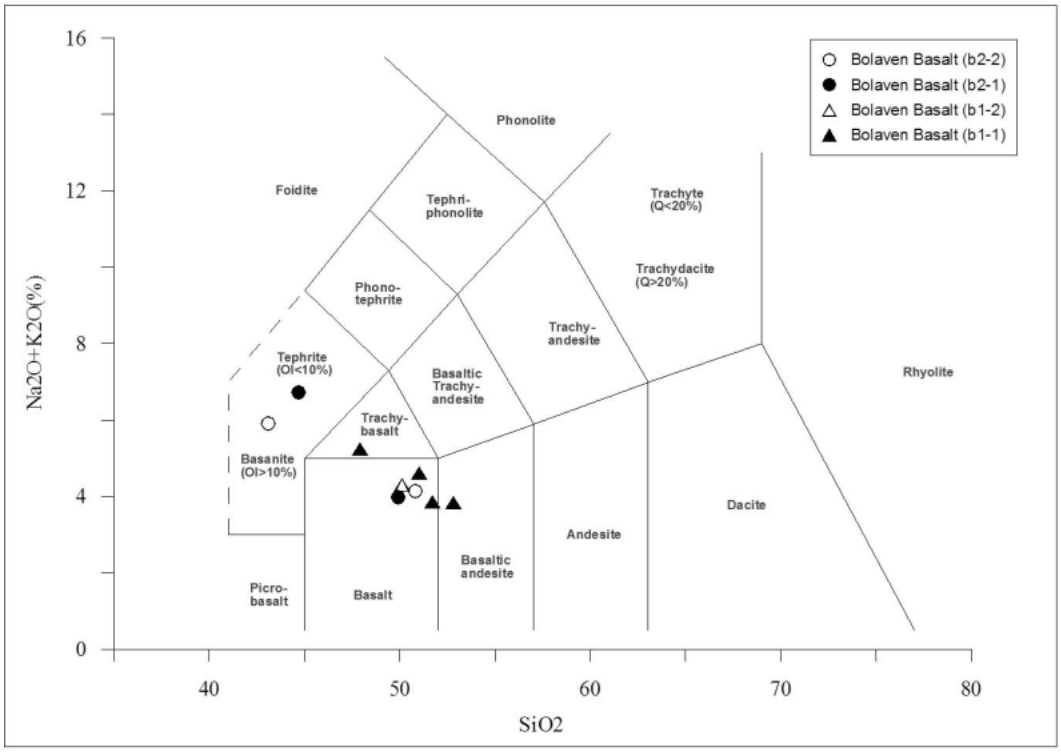

Figure 4.8.8 TAS discrimination diagram of basaltic rocks

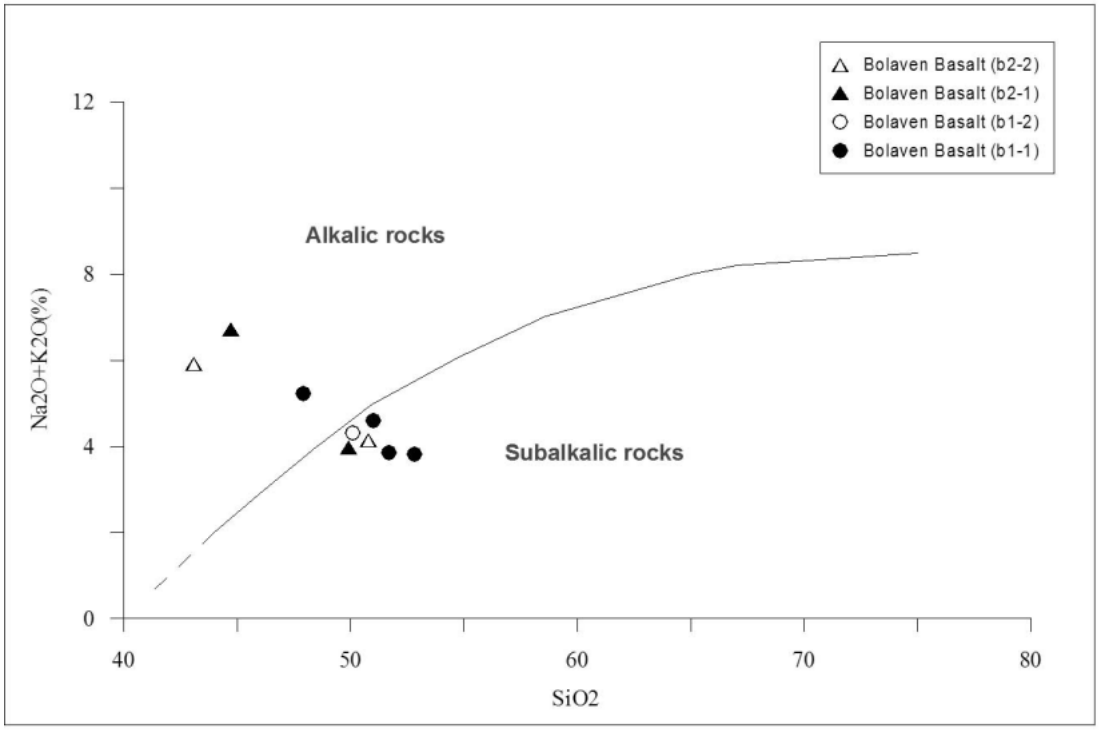

Figure 4.8.9 Alkali-silica diagram of basaltic rocks

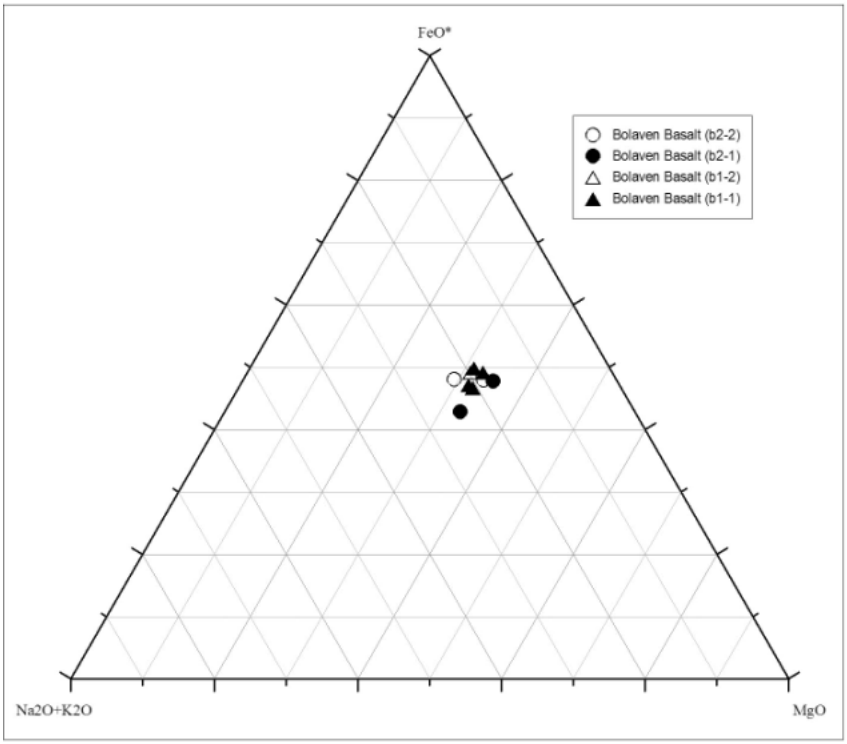

Figure 4.8.10 AFM diagram of basaltic rocks

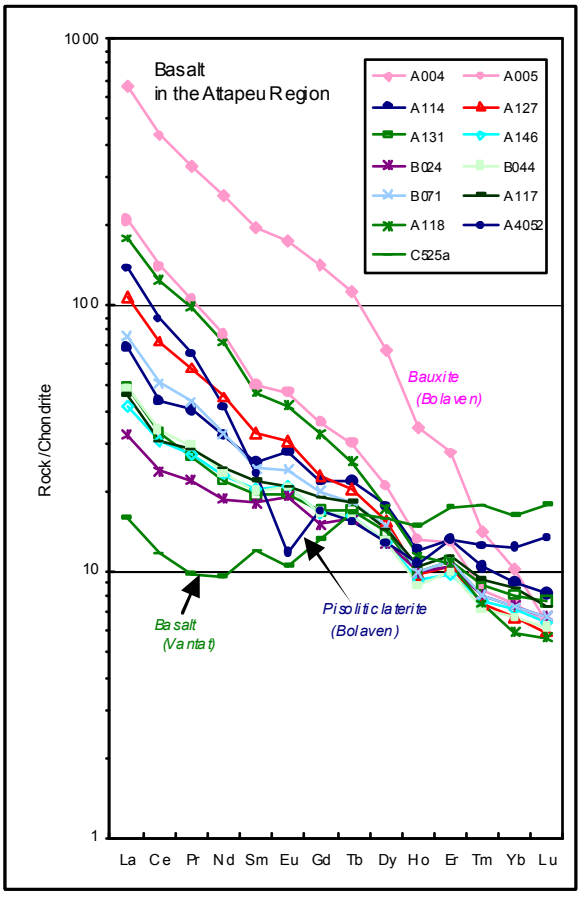

Figure 4.8.11 MORB normalized spider diagram of the basaltic rocks

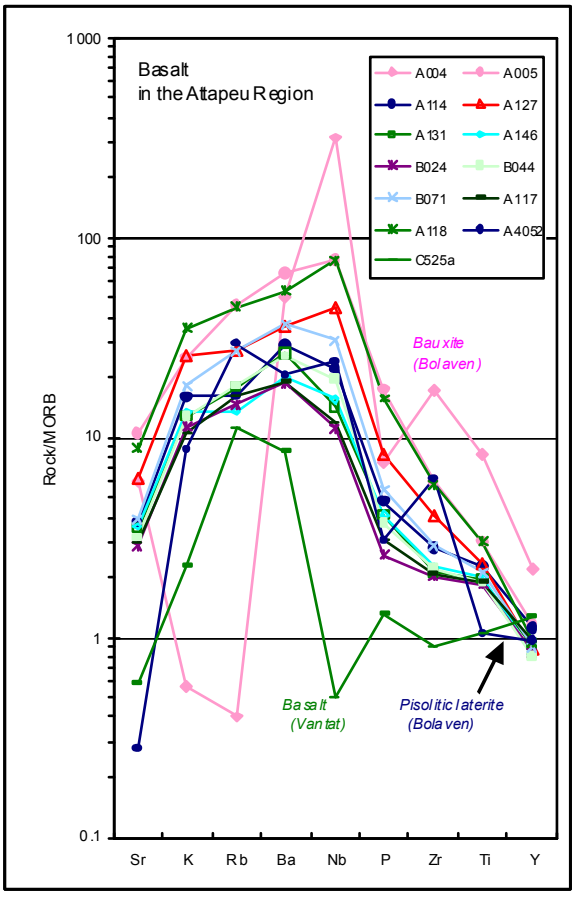

Figure 4.8.12 Chondrite normalized geochemical patterns of the basaltic rocks

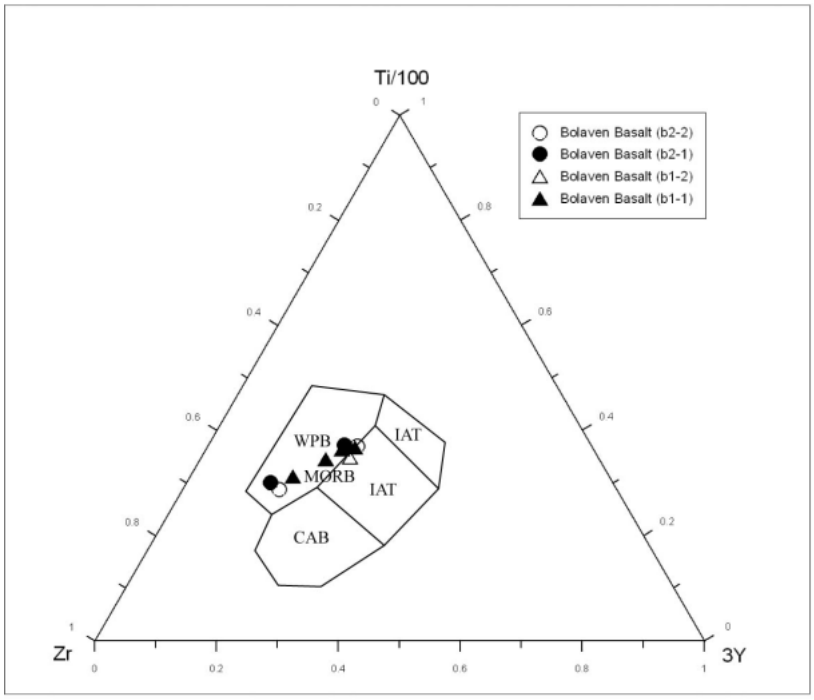

WPB, within-plate basalt;
CAB, island-arc calc-alkaline basalt;
IAT, island-arc tholeiite

Figure 4.8.13 Y-Ti-Zr discrimination diagram of basaltic rocks

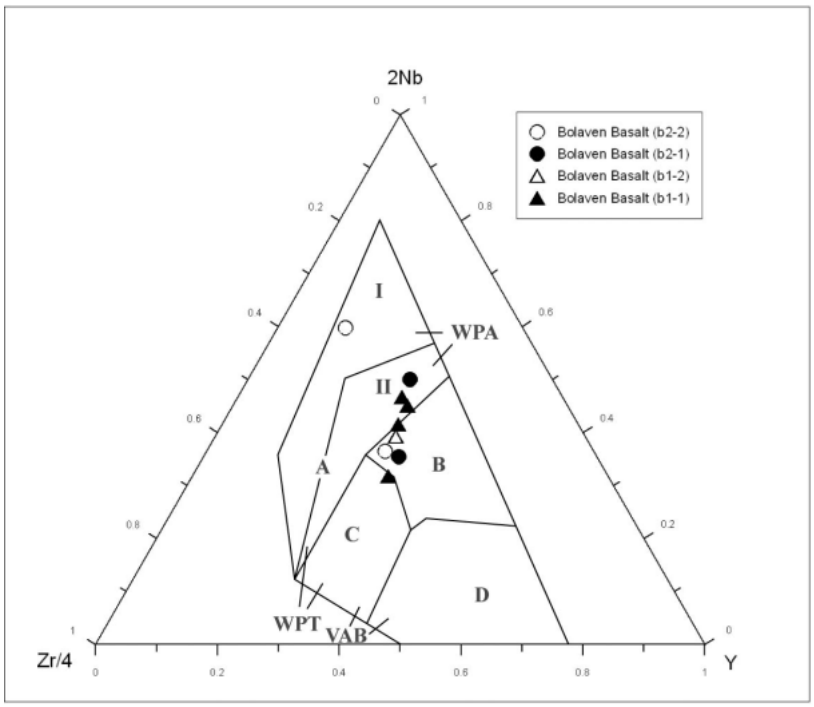

AI, within-plate alkali basalts; AII, within-plate alkali basalts and within-plate tholeiites;
B, E-type MORB; C, within-plate tholeiites and volcanic-arc basalts;
D, N-type MORB and volcanic-arc basalts
WPA, within-plate alkali basalt; WPT, within-plate tholeiite, VAB, volcanic-arc basalt

Figure 4.8.14 Y-Nb-Zr discrimination diagram of basaltic rocks

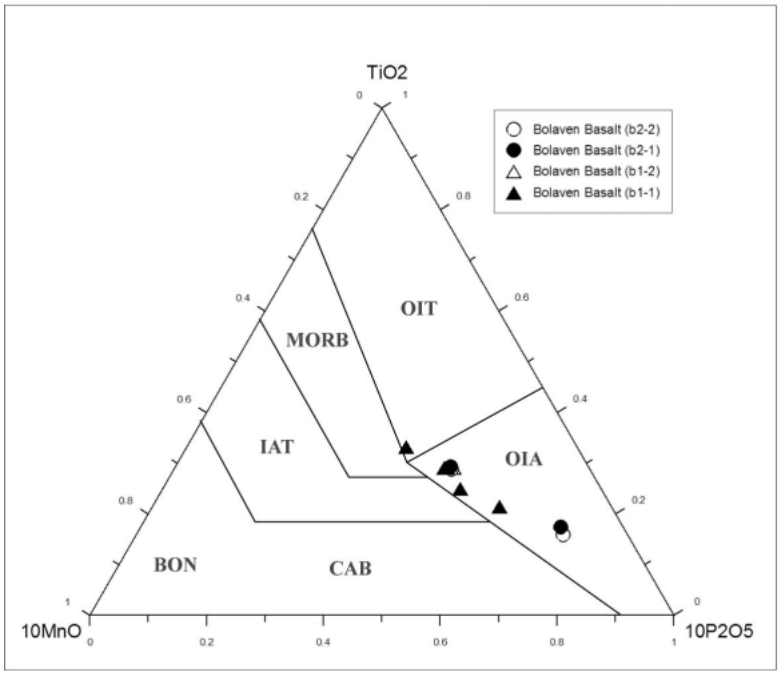

OIT, ocean-island tholeiite or seamount tholeiite;
OIA, ocean-island alkali basalt or seamount alkali basalt;
CAB, island-arc calc-alkaline basalt;
IAT, island-arc tholeiite; BON, boninite

Figure 4.8.15 P-Ti-Mn discrimination diagram of basaltic rocks

4.8.4 Chemical Analyses of Ore Samples

Chemical analyses were conducted for the ore samples collected during the geological survey (1:200,000 scale) of the second and third surveys. The analytical work was carried out at DGEO as a part of technical transfer.

1) Analyzed Samples

The chemical analyses were conducted for 48 samples as shown in Annex.10.

2) Contents and Method of Chemical Analyses

Chemical analyses of 8 elements such as Au, A, Cu, Pb, Zn, Ni, Mn were conducted by Atomic Absorption Spectrometer (AA-6300, Shimadzu Corp, Japan) at DGEO.

3) Analytical Results

The analytical results were shown in Annex.10.

Au, Cu, Pb and Ag show relatively high concentration in some of the samples. High concentration of Au, ranging from 0.68 to 2.56ppm, was obtained from the quartz veins collected in pelitic schist in the gold mine of army concession and in slate in the area of the Xe Xou River. Au concentrations much high than these were obtained for the quartz veins collected in the gold mine of army concession, but for the confirmation of Au concentration re-analysis of these samples are now in-progress. High Cu contents of 7,350ppm was obtained from the sample of sandstone with malachite-azurite dissemination collected from Triasic-Jurasic sandstone formation in eastern part of Xe Kong city. Cu content of 3,161ppm was obtained from quartz veins collecetd in the Gold Mine operated by the Army. High Pb contents of 2,281 was obtained from the samples of quartz hosted by slate in eastern part of the Ban Tat Noi Village, north of the gold mine of army concession. High content of Ag, 157ppm, also, was obtained from this quartz vein.

4.8.5 Magnetic Susceptibility

Measurement of magnetic susceptibility was conducted for all the 152 samples collected during the geological survey (1:200,000 scale) in the second and third surveys. By measuring magnetic susceptibility, it is possible to know an approximate amount of magnetic minerals included in rock. One of the classifications of granitic rocks, either magnetite series or ilmenite series, is based on an amount of magnetite included in the granitic rocks. The magnetic susceptibility acquired at the consolidation stage of magma can be easily changed during the episode of the secondary alteration and mineralization, therefore magnetic susceptibility can be an good indicator to know intensity of alteration and mineralization of particular rock.

The measurement of magnetic susceptibility was conducted during field work as a part of technical transfer.

1) Measured Samples

The measurement of magnetic susceptibility was conducted for 152 rock and ore samples as shown in Table 4.8.1.

2) Methods of Measurement

The measurement was conducted using KT-9 Kappameter (Exploranium G.S. Canada). Since rock and ore samples used for measurement have different sizes and the surfaces of them are not smooth, the measurement was done using Pin mode so that reshaping of the samples is not necessary. The value of magnetic susceptibility separating the magnetite and ilmenite series of the granitic rocks is $100x\ 10^{-6}$ emu/g, which correspond to 3.1 ($x10^{-3}$) in SI unit of KT-9 Kappameter.

3) Results

The results of measurements are given in Table 4.8.1.

The granitic rocks are separated in two groups, the one with high magnetic susceptibility of more than 3.0 and the other with low susceptibility of around 1.0. The former with higher magnetic susceptibility is considered to be magnetite series of granitic rocks, and hornblende-biotite granodiorite distributed along Route 18B and in the area of Xe Kaman Rivers and biotite-hornblende-quartz diorite belong to this group. The granitic rocks belong to the latter group with lower magnetic susceptibility are biotite granite-granodiorite distributed in the area of Xe Kaman River and biotite-hornblende granodiorite and two mica granite in the area of Xe Xou River.

The metamorphic rocks, sedimentary rocks, altered rock and the country rocks of mineralization show a low magnetic susceptibility of less than 1.0. The basaltic rocks generally have a high magnetic susceptibility of around 2.0 to 8.0 at maximum.

Table 4.8.1 Results of magnetic susceptibility measurement of granites and basalts

Ser. No.	Sample No.	Rock & Ore Name	Magnetic Susceptibility (*10^{-3} SI)	Ser. No.	Sample No.	Rock & Ore Name	Magnetic Susceptibility (*10^{-3} SI)	Ser. No.	Sample No.	Rock & Ore Name	Magnetic Susceptibility (*10^{-3} SI)	Ser. No.	Sample No.	Rock & Ore Name	Magnetic Susceptibility (*10^{-3} SI)
1	B001	Conglomerate	0.01	41	B041	Schist	0.15	81	B081	Granodiorite	5.46	121	B121	Basalt	2.03
2	B002	Sandstone	0.02	42	B042	Basalt	0.75	82	B082	Sandstone	0.01	122	B122	Basalt	2.54
3	B003	Sandstone	0.06	43	B043	Granodiorite	1.95	83	B083	Diorite	0.09	123	B123	Basaltic andesite	2.33
4	B004	Siltstone	0.09	44	B044	Basalt	1.21	84	B084	Diorite	2.30	124	B124	Basalt	1.34
5	B005	Sandstone	0.17	45	B045	Sandstone	0.00	85	B085	Quartz diorite	11.70	125	B125	Basalt	1.53
6	B006	Sandstone	0.26	46	B046	Sandstone	0.20	86	B086	Granodiorite	3.95	126	B126	Basalt	1.25
7	B007	Sandstone	0.18	47	B047	Siltstone	0.12	87	B087	Granodiorite	6.23	127	B127	Basalt	1.56
8	B008	Mudstone	0.10	48	B048	Shale	0.14	88	B088	Granodiorite	52.30	128	B128	Ignimbrite	0.09
9	B009	Schist	0.01	49	B049	Shale	0.23	89	B089	Diorite	5.82	129	B129	Ignimbrite	0.16
10	B010	Meta sandstone	9.51	50	B050	Sandstone	0.06	90	B090	Quartz vein	0.05	130	B130	Basalt	1.59
11	B011	Rhyolite	0.03	51	B051	Sandstone	0.01	91	B091	Gneiss	0.14	131	B131	Basalt	4.38
12	B012	Ignimbrite	0.05	52	B052	Siltstone	0.13	92	B092	Gneiss	0.12	132	B132	Granodiorite	1.84
13	B013	Ignimbrite	0.03	53	B053	Basalt	1.57	93	B093	Quartz diorite	0.32	133	B133	Granodiorite	1.65
14	B014	Sandstone	0.08	54	B054	Ignimbrite	0.07	94	B094	Granodiorite	4.79	134	B134	Mylonite	0.40
15	B015a	Sandstone	0.07	55	B055	Siltstone	0.00	95	B095	Granodiorite	0.21	135	B135	Schist	-0.06
16	B016	Mylonite	0.12	56	B056	Arkose sandstone	0.25	96	B096	Gneiss	-0.08	136	B136	Meta sandstone	0.07
17	B017	Granodiorite	0.06	57	B057	Sandstone	0.11	97	B097	Basalt	1.15	137	B137	Sulfide ore	0.64
18	B018a	Marble	0.04	58	B058	Sandstone	0.13	98	B098	Dacite	2.25	138	B138	Meta sandstone	0.03
19	B019	Granodiorite	4.95	59	B059	Sandstone	0.08	99	B099	Granodiorite	0.04	139	B139	Quartz vein	-0.06
20	B020a	Sandstone	0.01	60	B060	Sandstone	0.16	100	B100	Slate	0.03	140	B140	Gneiss	-0.01
21	B021	Mudstone	0.04	61	B061	Slate	0.05	101	B101	Conglomerate	-0.17	141	B141a	Quartz vein	-0.12
22	B022	Conglomerate	0.01	62	B062	Slate	0.02	102	B102	Granodiorite	30.30	142	B142a	Schist	0.20
23	B023	Mudstone	0.01	63	B063	Sandstone	0.02	103	B103	Syenite	0.05	143	B143	Quartz vein	-0.12
24	B024	Basalt	0.55	64	B064	Slate	0.03	104	B104	Granite	1.06	144	B144	Quartz vein	-0.10
25	B025	Sandstone	0.06	65	B065	Basalt	2.51	105	B105	Quartz vein	-0.15	145	B145	Quartz vein	-0.13
26	B026	Granodiorite	0.01	66	B066	Basalt	2.17	106	B106	Conglomerate	0.06	146	B146	Slate	0.02
27	B027	Granodiorite	6.85	67	B067	Quartz arenite	0.01	107	B107	Chert	-0.19	147	B147	Mylonite	0.28
28	B028	Granodiorite	1.62	68	B068	Dacite	0.01	108	B108a	Schist	0.02	148	B148	Basalt	2.07
29	B029	Gneiss	0.15	69	B069	Basalt	0.92	109	B109a	Chert	-0.08	149	B149	Basalt	1.98
30	B030	Andesite	0.05	70	B070	Dacite	0.03	110	B110	Limestone	-0.04	150	B150	Basalt	4.46
31	B031	Quartz vein	0.00	71	B071	Basalt	5.09	111	B111	Ignimbrite	-0.03	151	B151	Basalt	2.90
32	B032	Quartz vein	0.07	72	B072	Quartz arenite	0.02	112	B112	Quartz arenite	0.26	152	B152	Basalt	8.09
33	B033a	Quartz vein	0.02	73	B073	Quartz arenite	0.03	113	B113	Schist	0.03				
34	B034a	Quartz vein	0.15	74	B074	Quartz arenite	0.01	114	B114	Quartzite	-0.07				
35	B035	Sandstone	0.11	75	B075	Adamellite	0.02	115	B115	Basalt	0.72				
36	B036	Andesite	0.02	76	B076	Conglomerate	0.04	116	B116	Basalt	1.02				
37	B037	Schist	0.04	77	B077	Sandstone	0.01	117	B117	Basalt	1.96				
38	B038	Quartz arenite	0.04	78	B078	Granite	0.01	118	B118	Basalt	6.95				
39	B039	Meta sandstone	0.09	79	B079	Ignimbrite	0.03	119	B119	Conglomerate	0.00				
40	B040	Dacitic tuff	0.05	80	B080	Granodiorite	0.27	120	B120	Goethite	0.54				

4.8.6 Fluid Inclusion Studies

The fluid inclusion studies were conducted for the quartz samples with mineralization collected during the geological survey (1:200,000 scale) in the second and the third surveys.

Mineral showings are found in many locations in the area. For understanding the environment of ore genesis, including temperature of ore formation and nature of ore forming solution, homogenization temperature and salinity of the fluid inclusion of quartz included in ore samples and quartz veins were measured.

1) Studied Samples

The fluid inclusion study was conducted for 10 samples as shown in Table 4.8.2.

2) Methods of Measurements

The measurements of homogenization temperature and salinity of the fluid inclusion were conducted by microscope of LINKAM with heating and cooling system of LK-600PS at DOWA TECHNO RESEARCH, Japan.

3) Results of Studies

The results of measurements are show in Table 4.8.2.

The quartz veins in the schist of the gold mine of army concession (B139, B141a, B141b, B143, B144 and B145), where relatively clear mineralization was observed, and that in slate of the Xe Xou River area (B034a) give homogenization temperature ranging from 119 to 297 degree C. and salinity of 2.57 to 6.74 wt%. The average values of homogenization temperature and salinity on each sample basis are, respectively, 156.3 to 220.0 degree C. and 3.71 to 5.98wt%.

Table 4.8.2 Results of fluid inclusion measurement

Ser. No.	Sample No.	Coordinate (UTM)		Description	Temperature (℃)			Salinity (wt.%NaCl)		
		EW	NS		Number	Range	Average	Number	Range	Average
1	B031	761128	1638824	Quartz vein (w:5m) with green Cu in muscovite schist.	1	110	110	1	0.53	0.53
2	B034a	762011	1636821	Pyrite bearing quartz vein (intense pyritization) in shear zone of phyllite.	12	186-222	204.5	12	4.34-5.41	4.88
3	B078	736022	1654653	Quartz vein in massive biotite granite.	12	142-207	167.8	12	3.87-6.01	4.63
4	B090	740863	1668883	Quartz vein in migmatite zone.	11	156-214	184.3	11	4.03-6.30	4.85
5	B139	764079	1651645	Pyrite bearing quartz vein in biotite gneiss.	11	119-297	220.0	11	4.49-6.74	5.98
6	B141a	759036	1656418	Quartz vein (w:80cm) in muscovite schist at Au mine of military concession.	13	142-205	173.0	13	5.26-6.16	5.73
7	B141b	759036	1656418	Quartz vein (w:80cm) in muscovite schist at Au mine of military concession.	8	131-203	165.0	8	4.65-6.45	5.72
8	B143	759036	1656418	Quartz vein (w:80cm) in muscovite schist at Au mine of military concession.	7	144-189	163.7	7	4.34-5.56	4.95
9	B144	759014	1656444	Quartz vein (w:140cm) in muscovite schist at Au mine of military concession.	4	131-178	156.3	4	4.18-4.65	4.42
10	B145	759150	1656100	Quartz vein with barite (w:15cm) in biotite schist	9	126-248	188.7	9	2.57-4.96	3.71
11	B539a	738892	1641559	Quartz vein in trench	3	132-146	140.3	3	2.74-7.86	5.08
12	B554	741742	1636814	Quartz network, sericite alteration, Azurite, Malchite, Chlcopyrite, bonite and tenolite	6	136-214	184.7	6	3.23-9.86	12.71
13	B561	741289	1637442	.Qz.vein (10cm) with Malc.	3	158-165	161.3	3	6.01-6.45	6.25
14	B562a	741307	1537444	Quartz stockwork with Malc.diss.(w:5m<), sericite and silicification (strong)	2	198-204	201.0	2	6.3-7.31	6.80
15	C538	765302	1681353	Quartz vein with disseminated pyrite	9	151-176	163.9	9	5.86-7.73	6.64

The homogenization temperatures obtained in the Attapeu Area are within the range of the temperature of precipitation of quartz in the veins formed in the epithermal environment (170 to 230 degree). The typical epithermal gold deposit of Japan (e.g Hishikari and Kushikino deposits) have salinity of around 1 wt%, while fluid inclusions of the Victoria Mine, a typical epithermal deposit in Philippine, have salinity of 0 to 4.2wt% (homogenization temperature: 200 to 260 degrees C.). The salinities of fluid inclusion obtained in the Attapeu Area are similar to or slightly higher than these of the typical epithermal deposits.

4.8.7 Dating

Rock samples to be assayed dating were granitic rocks and basaltic rocks taken from geological mapping of scale 1/200,000 and 1/10,000 during second to sixth field survey.

Effusive and emplacement phases of igneous rocks and alteration phases of rocks related to deposits were clarified by dating.

1) Method of Analysis

K-Ar dating analysis was conducted by ActLabs Ltd., Canada and Ar-Ar dating analysis was conducted by Hiruzen Geochronology Research Institute Ltd., Japan.

2) Analytical Result

K-Ar dating result is shown in Table 4.8.3 and Ar-Ar dating result is shown in Table 4.8.4.

Table 4.8.3 Results of K-Ar dating of granitic rocks and basaltic rocks

Ser. No.	Sample No.	Coordinate (UTM) EW	Coordinate (UTM) NS	Rock Name	K-Ar dating	Estimate Age	%K	$^{40}Ar_{rad}$, nl/g	% $^{40}Ar_{air}$	Age (Ma)	Age	Remarks
1	A153	769685	1636008	Two-mica GR	biotite	Permian to Triassic	5.44	68.077	1.5	301.5+7.7	Carboniferous	Loc.01A464 Xe Kaman (upstream)
2	B081	737580	1655897	Hbl.Bio.GD	biotite	Carboniferous	2.71	45.84	2.4	396.6±10.4	Devonian	Loc.01B293 Xe Kaman (middle)
3	B088	738498	1668467	Bio.Px.Hbl.DI	hornblede	Permian to Triassic	0.54	8.389	9.2	367.3+9.6	Devonian	Loc.01B316 Xe Kaman (middle)
4	B531	745065	1636793	Bio.Hbl.GD	whole rock (× hornblende)	Permian to Triassic	1.83	18.871	5.4	252.0±6.5	Permian	Loc.03B196 Area A
5	B546	760488	1638836	Bio.Hbl.GD	amphibole (× hornblende)	Permian to Triassic	n.d.***	6.429	15.1	n.d.	n.d.	Loc.03B302 Area B
6	B134	740337	1640961	Mylonite	sericite (muscovite)	Permian to Triassic	4.07	46.46	3.5	277.0+7.1	Permian	Loc.01B054 Area A&D (Route 18B)
7	B147	759162	1656212	Mylonite	whole rock (× muscovite)	Permian to Triassic	0.58	4.325	21.3	185.7+5.0	Jurassic	Loc.02B159 Army Mine
8	A117	628448	1690054	Ol.BA lava	whole rock	Neogene	0.64	0.212	89.8	8.7+0.4	Tertiary	Loc.01A373 Bolavene
9	A127	618039	1683025	Px.BA lava	whole rock	Neogene	1.59	7.611	12.2	121.4+3.1	Cretaceous	Loc.01A393 Bolavene
10	B044	728088	1665289	Px.BA lava	whole rock	Neogene	0.72	1.111	71.9	40.0+1.3	Tertiary	Loc.01B155 northern Xe Kaman (north of Paam)
11	C520	740800	1637132	Two-mica GR	whole rock (× muscovite)	Carboniferous	0.05	0.708	84	364.2+13.4	Devonian	Loc.04C041 Army Mine
12	C525a	758430	1656200	Meta BA	whole rock	before Carboniferous	0.15	1.624	57.9	272.1+ 8.1	Permian	Loc.04C046 Army Mine
13	B515	757929	1655788	Hbl.Bio.GD	biotite	Permian	1.82	18.77	18.9	251.6±6.5	Permian	Loc.03B095 Area A

The K concentration was performed by ICP
The argon analysis was performed using the isotope dilution procedure on noble gas mass spectrometer.

Table 4.8.4 Results of Ar-Ar dating of granitic rocks

Ser. No.	Sample No.	Coordinate (UTM)		Rock Name	Ar-Ar dating	Estimate Age	Age (Ma)	Age	Remarks
		EW	NS						
1	A083	747911	1632403	Hbl.Bio.GD	biotite	Permian to Triassic	248.61±25.16	Permian	82.3% of ^{39}Ar released Loc.01A270 south of Area A
2	A083	747911	1632403	Hbl.Bio.GD	hornblende	Permian to Triassic	269.35±29.75	Permian	57.7% of ^{39}Ar released Loc.01A270 south of Area A
3	B099	748590	1669280	Heterogeneous Hbl.Bio.GD	biotite	Permian to Triassic	-33.25±11.65	-	Loc.02B015 west of Ban Tat Noi
4	B099	748590	1669280	Heterogeneous Hbl.Bio.GD	hornblende	Permian to Triassic	-6.96±9.35	-	Loc.02B015 west of Ban Tat Noi

The step heating was performed by argon ion laser.
The temperatures on heating was measured using infrared temperature indicator.
The argon analysis was performed using the isotope dilution procedure on noble gas mass spectrometer.

4.9 Geological Mapping of Detail Survey (1:10,000 scale)

The detail survey was conducted in the areas of high potentially for mineral resources selected on the bases of mineral showings and anomalies of stream sediments geochemical survey found by the geological mapping of 1:200,000 scale (Figure 4.9.1). Three areas from the Eastern Attapeu Area (Area A, Area B, Area D) (Figures 4.9.2 and 4.9.3) and one area from the Western Attapeu Area (Area C) (Figures 4.9.4 and 4.9.5), comprising total area of 84km^2, were selected for detail survey.

The geological mapping of the detail survey area was commenced during the fifth and sixth survey. Stream sediments geochemical survey is simultaneously conducted.

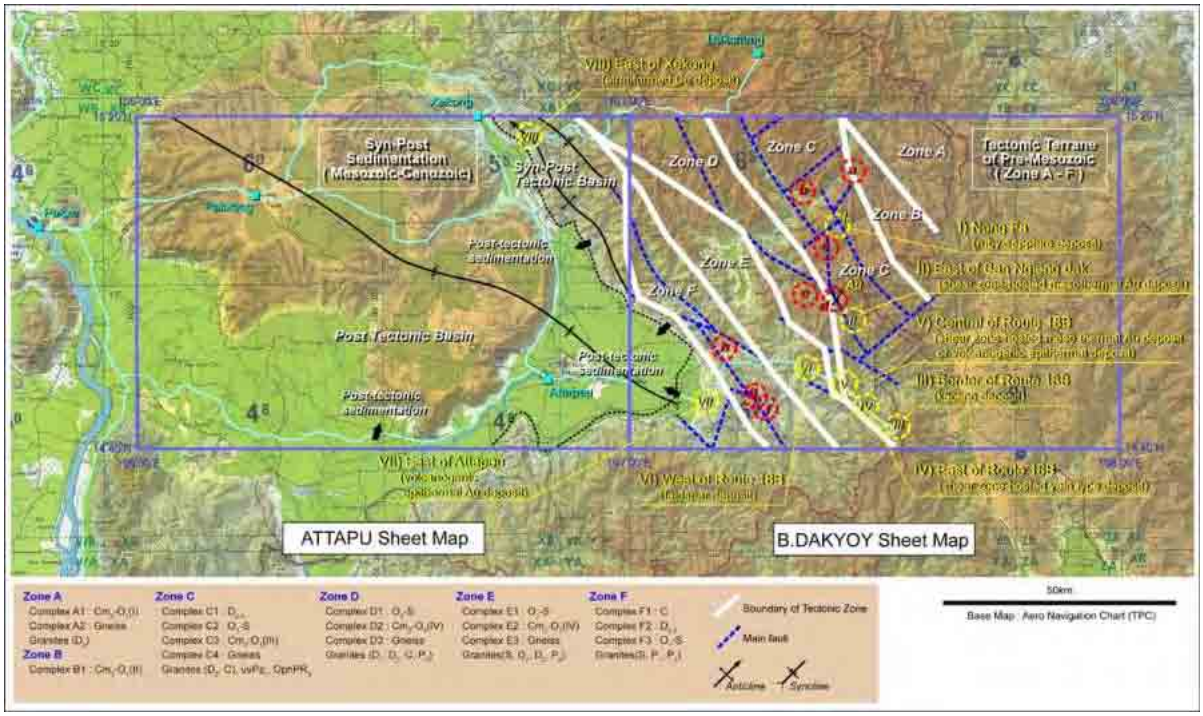

Figure 4.9.1 Location map of potential area for mineralization

The area A is located in the western part of the mountains existing in the eastern part of Attapeu City. The survey range is north-south 8km by east-west 8km. As the geochemical anomalies of gold by stream sediment are detected in this area, gold mineralization are expected in the area.

The area B is located at the sign 90km point on the National route 18B line in the mountains existing in the eastern part of Attapeu City. The survey range is north-south 4km by east-west 4km. As the quartz veins, pyrite dissemination, veinlet and sulphur leached are observed in the outcrop of the sign 90km point, the gold mineralization is expected.

The area C is located in the eastern part of Kong River flowing in northern end of the geological map sheet of the Attapeu area, and the area situates in the southeastern part of Xekong City. The survey range is north-south 4km by east-west 4km. As the copper minerals such as malachite and azurite are observed within the sandstone exposed on the road in the area, the copper mineralization is expected.

The area D is located in the western part of the mountains as well as the area A. The area D is adjoins the area A. The survey range is north-south 4km by east-west 4km. As the geochemical anomalies of gold by stream sediment are detected in this area, gold mineralization are expected in the area.

The objectives of the detailed geological survey are to understand the characteristics of mineralization, to grasp the scale of the ore deposits, and to create the ore genesis model. During field survey, in addition to the description of detail geology and mineralization, the densely sampling of stream sediment, the collection of ore samples in mineralized points, and their chemical analysis were carried out.

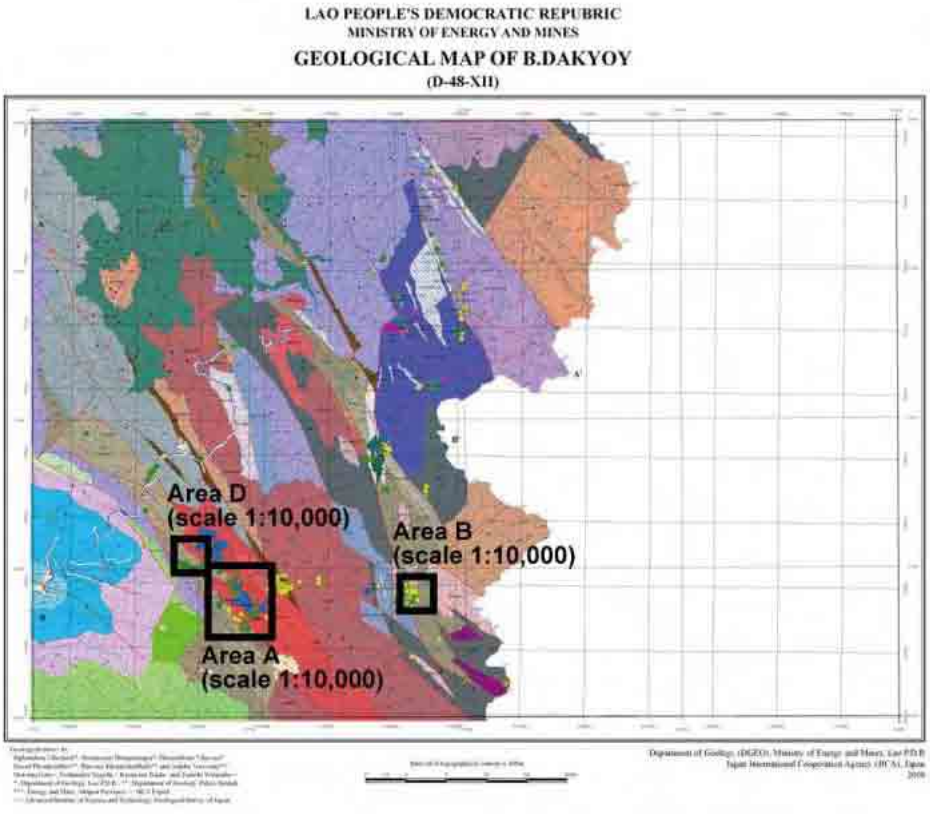

Figure 4.9.2 Location map of detail survey area of B.Dakyoy map sheet

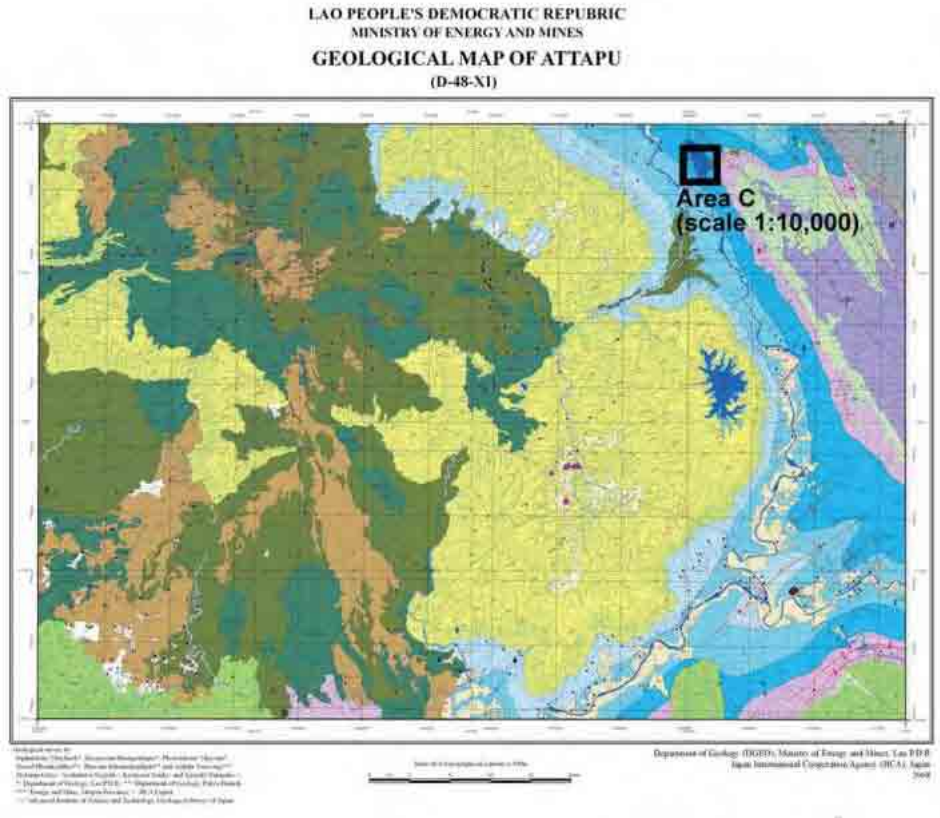

Figure 4.9.3 Location map of detail survey area of Attapeu map sheet

4.9.1 Area A

The Area A is located in south of the Ban May Phao Sauu Phanh Villager, which is located 50km east of Attapeu City (Figures 4.9.4, 4.9.5, 4.9.6, 4.9.7, 4.9.8 and 4.9.9). The area is located along so-called "Ho Chi Minh Trail" and Route 18B runs through east to west in northern part of the area. The Area A was selected because of Au and Cu anomalies found by the stream sediments geochemical survey conducted during the second and third geochemical survey.

Granitic rocks of probably Palaeozoic to Mesozoic age are distributed in the most of Area A and metamorphosed pelitic rocks and slate occur in western part of the area.

Three intrusive bodies of granitic rocks, elongated in northwest-southeast direction, occur in the area. They area:

- Medium to coarse, biotite-hornblende granodiorite
- Coarse biotite-hornblende quartz diorite-diorite
- Fine to medium, biotite-hornblende granodiorite-quartz diorite

Among these, medium to coarse, biotite-hornblende granodiorite dominantly occur, occupying most of the central part of the Area A. Coarse biotite-hornblende quartz diorite-diorite occurs northeast part of the Area A, and fine to medium, biotite-hornblende granodiorite-quartz diorite occur within medium to coarse, biotite-hornblende granodiorite as small bodies. Two granitic bodies of medium to coarse, biotite-hornblende granodiorite and fine to medium, biotite-hornblende granodiorite-quartz diorite have been partly undergone mylonitization.

Medium to coarse, biotite-hornblende granodiorite is in general homogeneous and becomes inhomogeneous and melanocratic at the vicinity of mylonite zone. The characteristic feature of this lithofacies is rectangular to wedge shaped hornblende of 2 to 5mm long. The hornblende occasionally shows a clear flow structure, and dome and basin structure by alignment of hornblende is locally observed.

Coarse biotite-hornblende quartz diorite - diorite is, as a whole, inhomogeneous rock and characteristically includes rectangular to wedge shaped hornblende of approximately 5mm long and glomeroporphyric biotite of 8mm across. In some part, abundant recrystalized biotite occurs and it forms melanocratic part, showing gneissose texture. The inhomogeneous gneissose part occasionally includes zenolith of dacite to granodiorite and chilled margin is observed in the matrix.

Fine to medium, biotite-hornblende granodiorite-quartz diorite is homogeneous. Characteristic lithological feature of this is that it is finer compared with compact, medium to coarse, biotite-hornblende granodiorite, and that coarse hornblende is not included and amount of quartz is less.

Mylonitized granitic rocks are fine grained and show preferred orientation of quartz and mafic minerals, shear-band and S-C structure. Bands of mylonitization are 10 to 20cm thick and schistosity occurs parallel to foliation of mylonite. The YZ plane of mylonite is elongated in NW-SE to NNW-SSE direction and this is parallel to oblique to the strike of schistosity of metamorphic rocks in surrounding area. The YZ plane dips approximately 80 degree to NW and NE. The mylonitized granite, in some part, gradually changes to quartz schist and muscovite quartz schist.

Distribution of metamorphic rocks is elongated in NW-SE direction, same as granitic rocks. The metamorphic rocks consists of quartz schist, muscovite-quartz schist, biotite schist, muscovite schist and slate. The metamorphic rocks contact with mylonitic medium to coarse biotite-hornblende granodiorite of granitic rocks on its eastern side and quartz schist and muscovite-quartz schist of metamorphic rocks occur at the contact.

In the area of metamorphic rocks, from east to west, rockfacies gradually change to quartz schist to muscovite quartz schist, biotite schist, muscovite schist and slate, and grade of metamorphism, as a whole, tend to decrease from east to west. The metamorphic rocks strike NE-SW, dipping 80 to NW or

SE. Alternation of biotite schist and muscovite schist is, occasionally, observed and it often forms fold structure of few meter long wavelength. The axis of fold plunge at around 40 degree in NW direction.

The main occurrences of mineralization found in the area are dissemination of malachite in the mylonite zone of granodiorite and foliated granite, quartz vein with malachite-chalcopyrite-pyrite and quartz vein with pyrite. Although all of these are only small scale mineralization observed on outcrop, since the mineralization occur along ductile fracture and schistosity, an extension of mineralization along the fracture zone is expected. The ductile fracture and schistosity strike in NW-SE direction.

The mineralization similar the porphyry type copper deposits is observed in the central part of the area. Size of mineralization is 5m to 10m in width. In the outcrops of granodiorite, the mineralization has the copper oxide minerals of malachite and azurite and develops the dissemination of chalcopyrite and bornite. And it is followed by the quartz network with the sericite alteration and the quartz veins with the dissemination of pyrite and chalcopyrite.

The mineralization was probably formed after the emplacement of granodiorite body accompanying with the porphyry type copper mineralization in-situ, and it was formed under the wrench tectonics caused mylonitization and cataclasitization.

In the two sites indicating the copper mineralized zones accompanying with the sericite alteration and quartz stockwork, the trench survey was carried out in order to detect the extension of mineralization. Sketching in the trench survey, the ore samples for chemical analysis and the rock samples for the identification of alteration minerals were collected from two trenches.

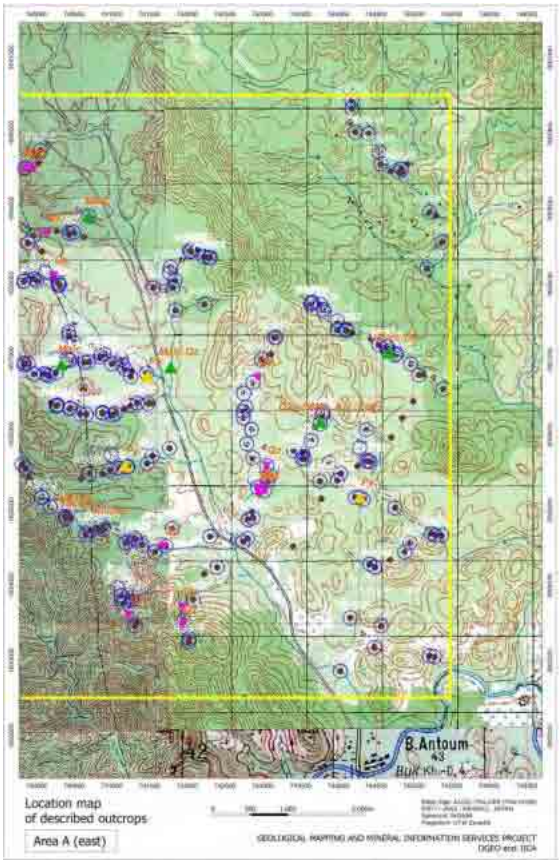

Figure 4.9.4 Topographic map of Area A (east)

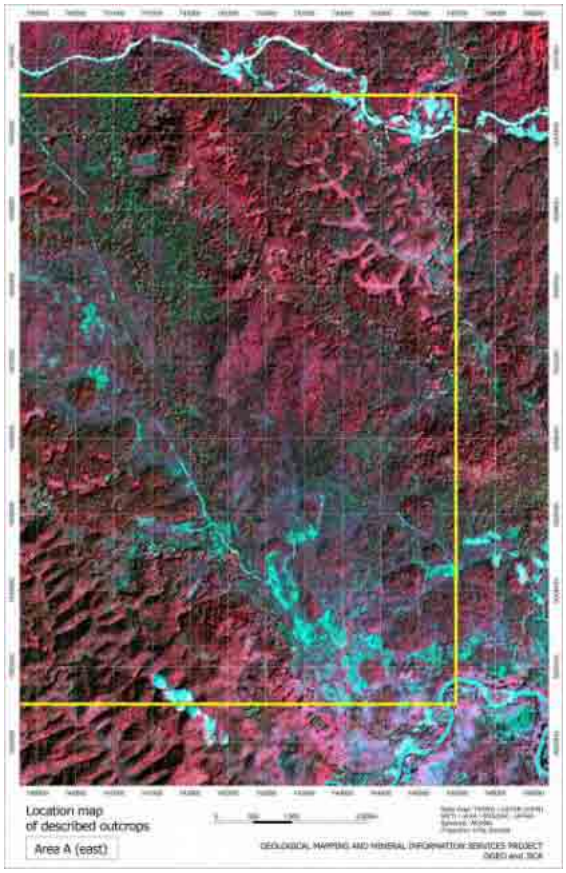

Figure 4.9.5 ASTER imagery map of Area A (east)

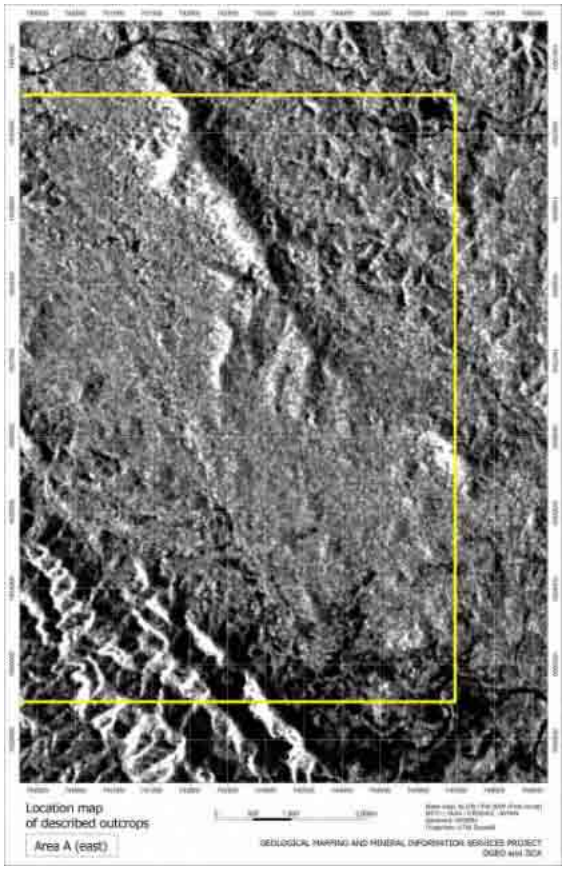

Figure 4.9.6 PALSAR imagery map of Area A (east)

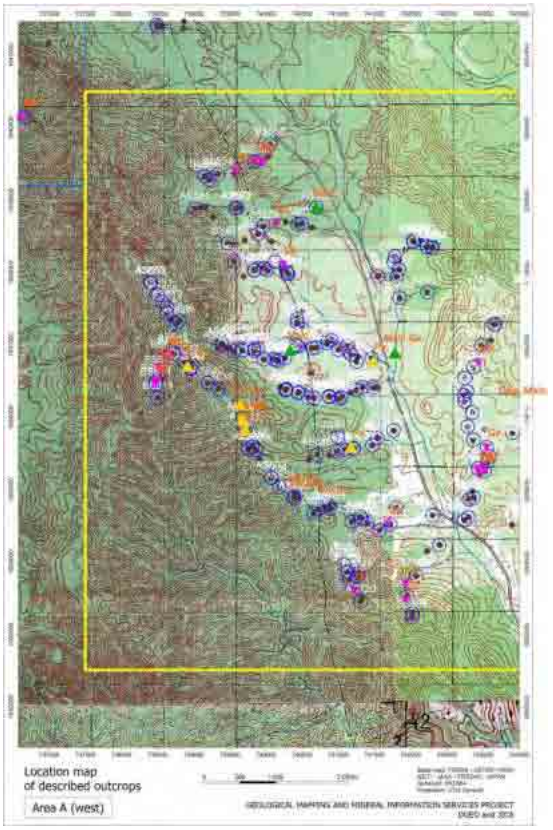

Figure 4.9.7 Topographic map of Area A (west)

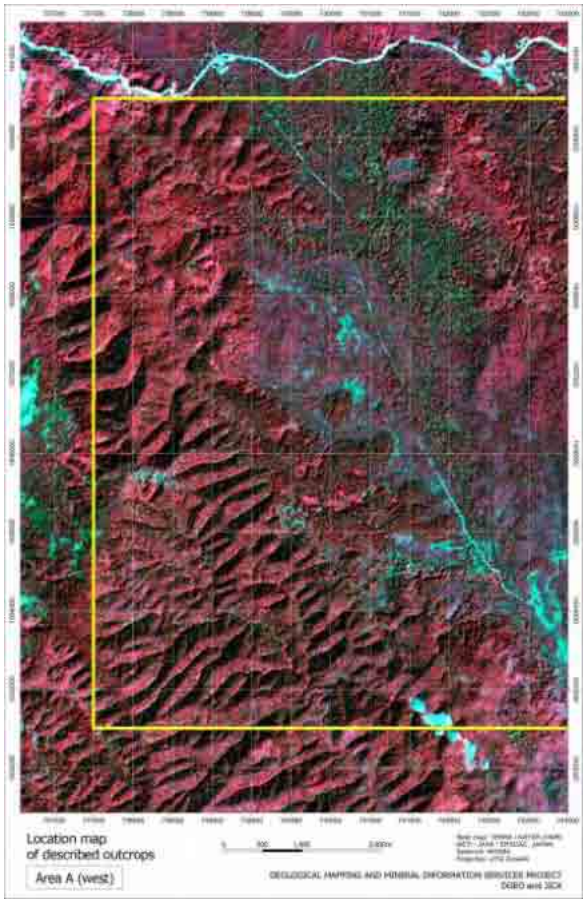

Figure 4.9.8 ASTER imagery map of Area A (west)

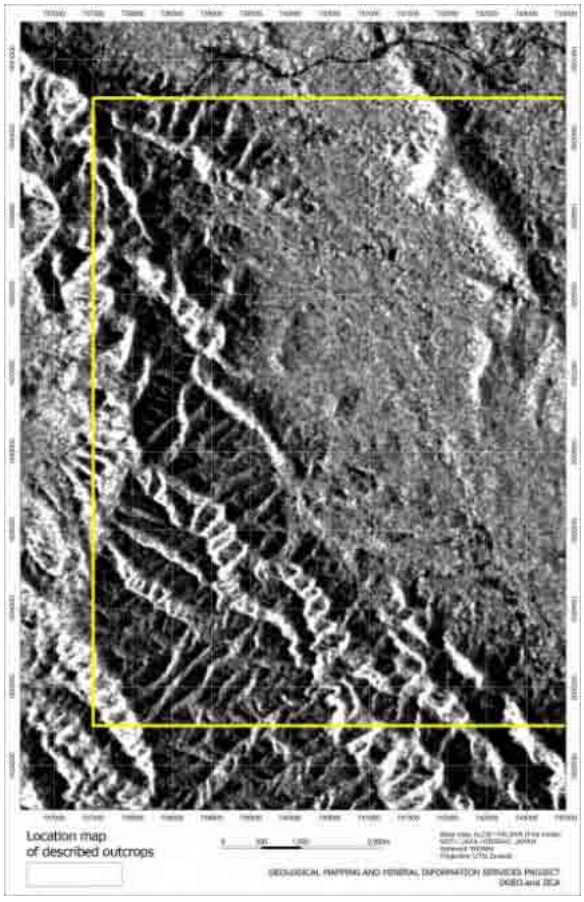

Figure 4.9.9 PALSAR imagery map of Area A (west)

4.9.2 Area B

The area B is located 25km east form Area A (Figures 4.9.10, 4.9.11 and 4.9.12). Route 18B runs northwest-southeast direction in the center part of the area. The reason for selection of this area for detail survey is that, during second and third surveys, pyrite disseminated epithermal alteration zone with brittle fracture and opalin quartz veins was found, and hydrothermal mineralization in the area is expected.

Most of the area is occupied by weakly metamorphosed rocks of the Paleozoic age, mainly consisting of slate, and pelitic schist, mainly consisting of muscovite schist, occur in the western part of the area.

The slate, dominant rock type of the weakly metamorphosed rocks, is distributed in a stretched zone elongated in NNW – SSE direction in the center of the area. It is dark to dark gray and original bedding of the alternation of sandstone and mudstone is well preserved. The bedding is nearly parallel to cleavage of slate. It strikes in NW –SE direction with high angle dip. The slate alternate with biotite schist near the northwest contact with pelitic metamorphic rocks.

Micro folding and minor faults are clearly observed in the slate. The minor faults strikes in NW – SE direction with high angle dip. Slip offset of these minor faults are normally few cm.

The pelitic schist mainly consists of muscovite schist and biotite schist, and it is distributed in elongated area in NNW –SSE parallel to the distribution of slate which occur to the east of pelitic schist. The contact between pelitic schist and slate is gradational and alternation of biotite schist and slate occur at the contact between slate and pelitic schist.

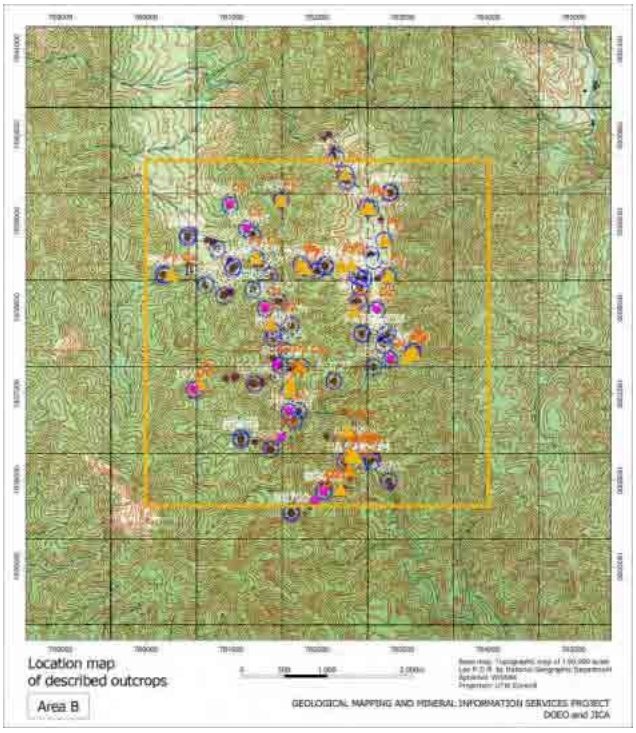

Figure 4.9.10 Topographic map of Area B

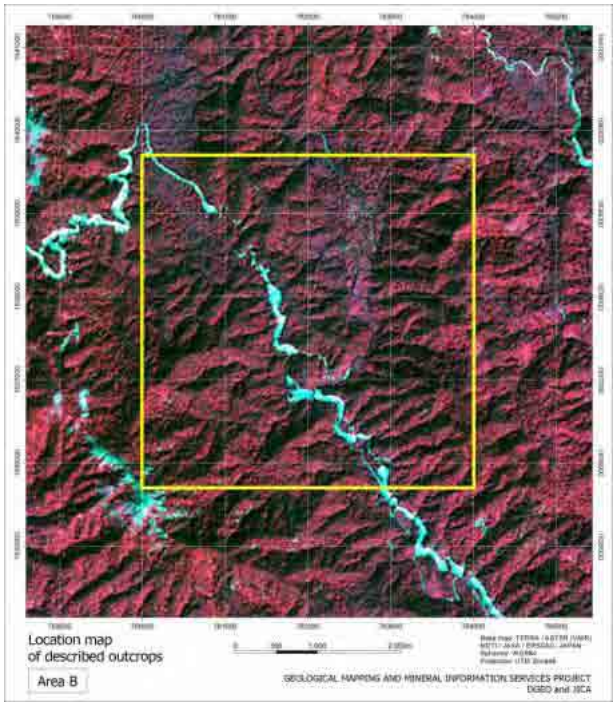

Figure 4.9.11 ASTER imagery map of Area B

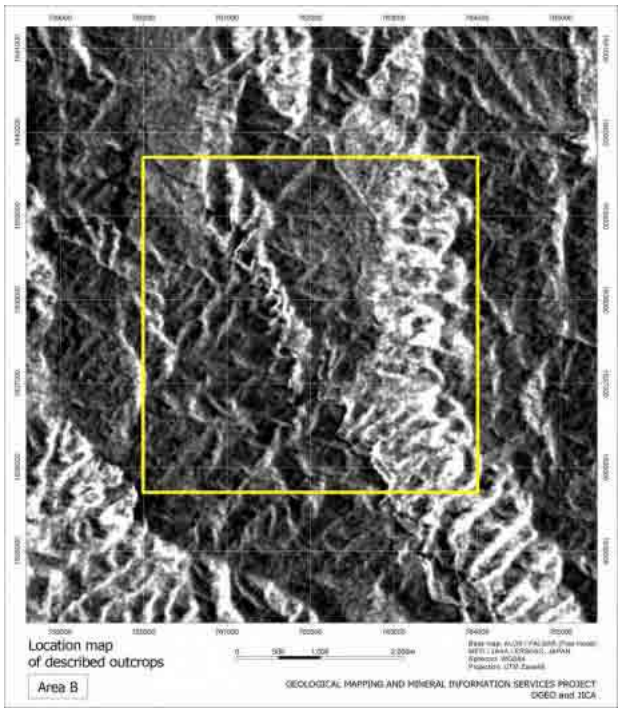

Figure 4.9.12 PALSAR imagery map of Area B

Brittle fractures zones were found in the slate of the center apart. They trend in NW –SE to N-S direction and, in many places in fracture zones, strong pyrite dissemination and stockwork veins of quartz were found. The fracture zone with mineralization together with fracturing, found along Route 18B, is 100m wide.

Main mineralization observed in the area is, above mentioned, pyrite bearing quartz stockwork veins in the fracture zone. Similar mineralization of 5m to 50m wide is found in several locations along the Route 18B and on river bed. Occurrences of this mineralization together with brittle fracture suggest that brittle fracture zone are genetically related to the mineralization.

4.9.3 Area C

The Area C is located on left side of the Xe Kong River, approximately 10km east of Xe Kong City (Figures 4.9.13, 4.9.14 and 4.9.15). The road connecting Xe Kong and Dakchung runs east-west direction in the center of the area. The reason for selection of Area C is to re-assess potentiality of the copper mineralization occurring in the Permian to Jurassic marine sediments.

The sandstones of Triassic to Jurassic, mainly consist of very fine sandstone and fine sandstone and alternation of calcareous sandstone and shale and muddy limestone are locally observed. Very fine sandstone is pale red to gray and fine sandstone is pale greenish gray to gray, and each bed of them few m thick forms alternation. They have NW–SE trend and dip 10 degree to west. The sandstone beds has a horizon including abundant shell fossils and this horizons can be traced for few kilometers.

Alternation of calcareous sandstone and shale and muddy limestone occur beneath the shell fossil rich sandstone horizon. They are gray to dark gray and hard. Muddy limestone includes acicular fragments, probably part of Mollusca. The alternation of calcareous sandstone and shale is well bedded and strike and dip are conformable to sandstone formation.

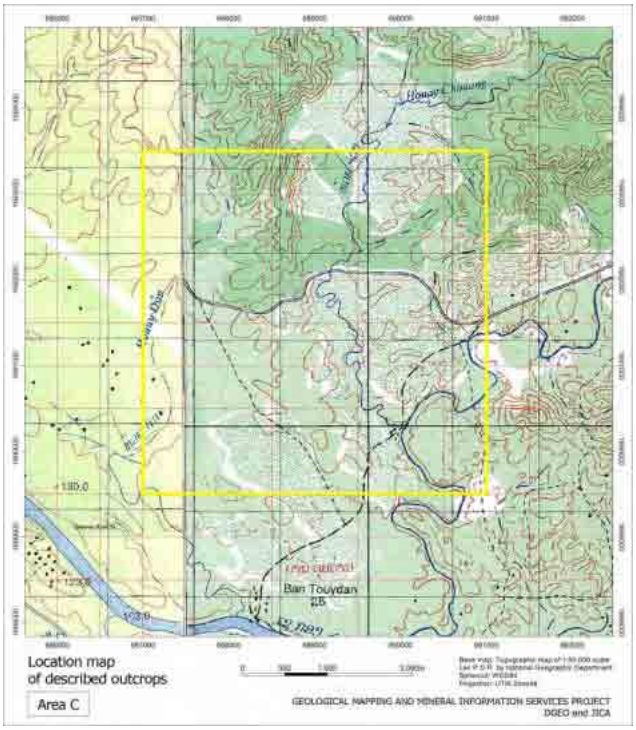

Figure 4.9.13 Topographic map of Area C

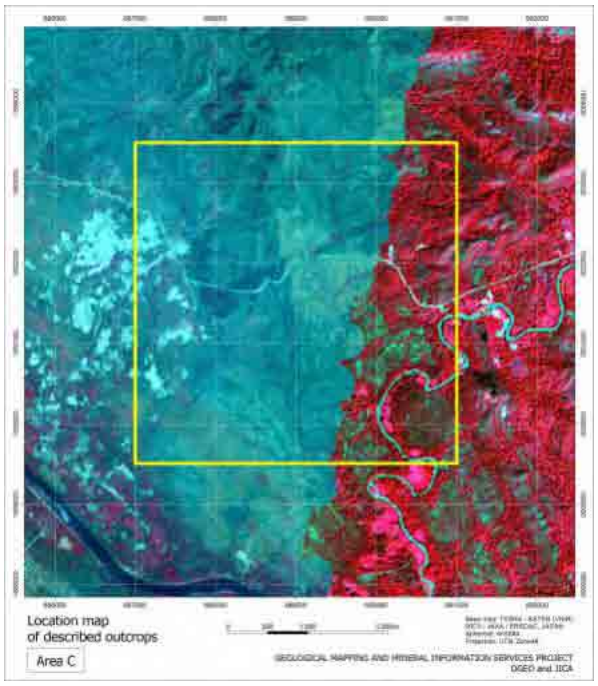

Figure 4.9.14 ASTER imagery map of Area C

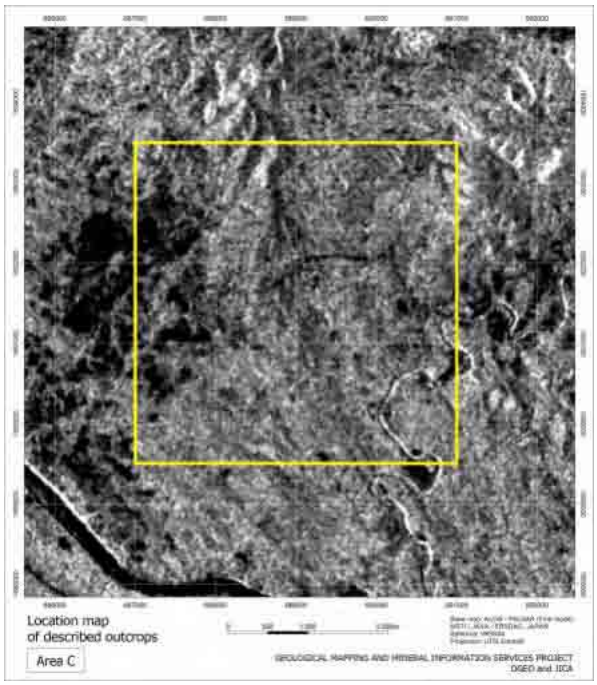

Figure 4.9.15 PALSAR imagery map of Area C

The Area C is located within the folding structure, at center of which Permian to Triassic rocks occur, and the area belongs to north west limb of the anticline. The axis of anticline strikes NW-SE direction and plunges to NW direction. The limbs of anticline generally decline gently, at 10 degrees to west and 20 degrees to east. The beds distributed in the area form the monoclinic structure striking north to south and gently dipping to west.

The mineralization found in the area shows occurrences of azurite and malachite in the sandstones. Disseminations of these are found along irregular fractures of small scale in the sandstones. Absences of alteration in the country rock suggest the type of mineralization in the area to be either strata-bound or epithermal type.

The host rock of the strata-bound type copper mineralization observed in the area is the calcareous sandstone with fossils of mollusk. The sandstone bed continues more than 4km from south end to north end in the area. The thickness of the bed is 10cm in south part, about 2m in central part and 1.5m in north part, and the continuity of the bed is very good. The horizon includes copper oxide minerals mainly consisting of malachite and accompanies with azurite and chalcopyrite in northern part of the area. The copper minerals such as malachite and azurite are observed in the thin beds of pale grey mudstone with the red mudstone bed.

4.9.4 Area D

The Area D is located in north west of Area A, north west of Ban May Phao Sauu Phanh Village and 50km east of Attapeu City (Figures 4.9.16, 4.9.17 and 4.9.18). The Route 18B runs in east-west direction in the center part of the area. The reason for selection of Area D is that anomaly areas of Au and Cu found by the stream sediments geochemical survey conducted in the second and third surveys.

The granitic rocks of Paleozoic to Mesozoic ages occur in the northwestern part of the area and metamorphosed mudstone and sandstone and slate occur in the central to western parts of the area. The conglomerate and sandstone occur in the southwestern part of the area, uncomformably overlying the metamorphic rocks.

The granitic rocks are distributed in an area elongated in north west-south east direction and medium to coarse biotite and hornblende granodiorite is main rock facies. It is the same rock facies to medium to coarse biotite and hornblende granodiorite of Area A and this lithological unit occurs continuously from Area A to Area D. Similar to Area A, the granitic rocks characteristically includes rectangular to wedge shape hornblende of 2 to 5mm across. Preferred orientation of hornblende is often observed and it locally forms dome and basin structure. Similar to the granitic rocks of Area A, the granitic rocks area was mylonitized.

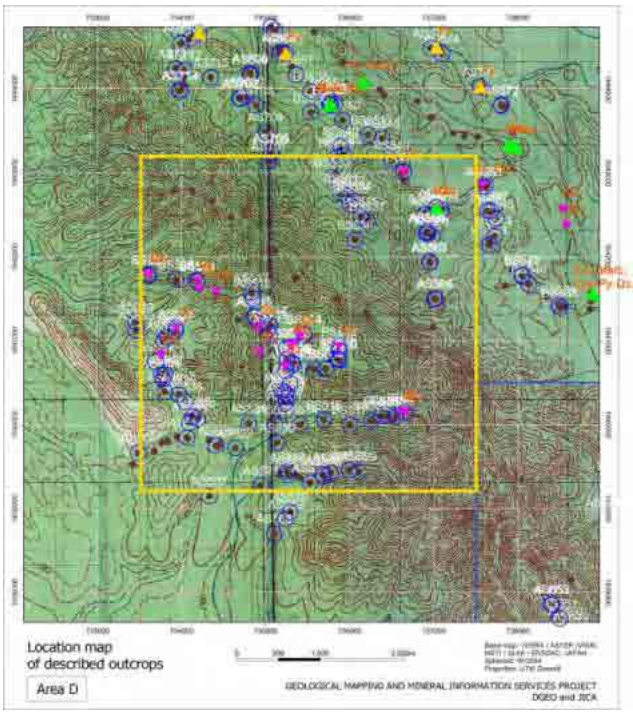

Figure 4.9.16 Topographic map of Area D

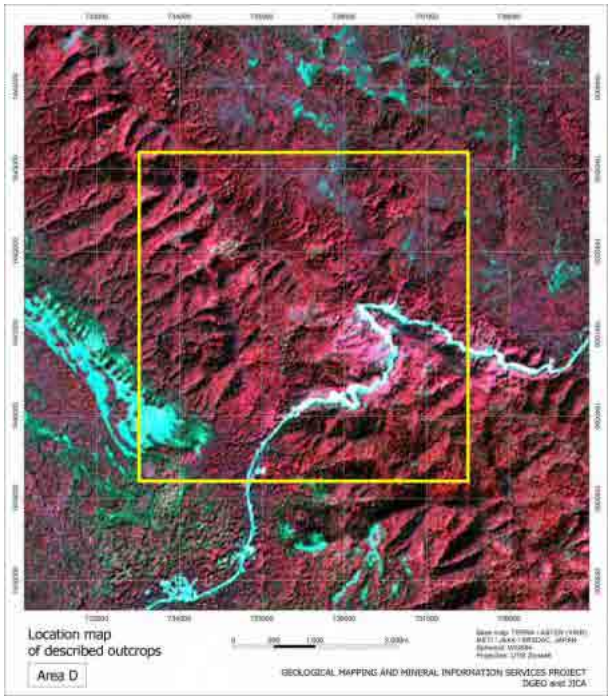

Figure 4.9.17 ASTER imagery of Area D

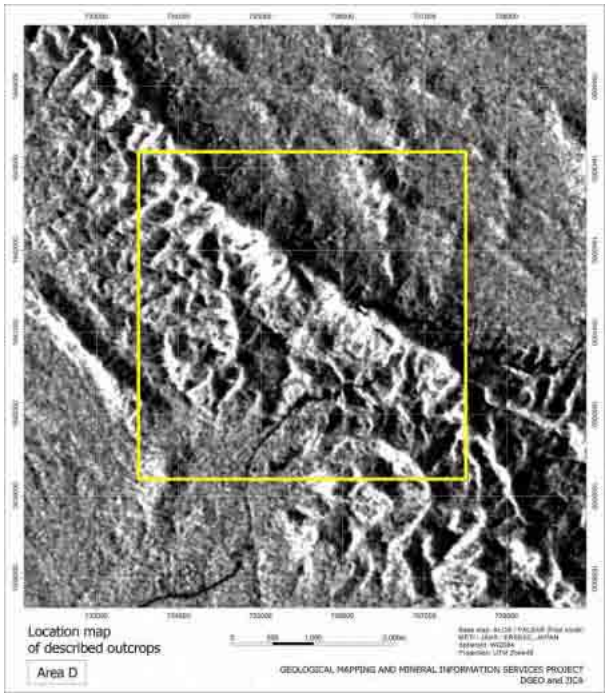

Figure 4.9.18 PALSAR imagery of Area D

The mylonitized granitic rocks are fine grained showing preferred orientation of quartz and mafic minerals, shear-band and S-C structure. The mylonite zones are 10 to 20m wide and schistosity parallel to the plain structure of mylonite occurs. YZ plain of the mylonite is elongated in NW-SE to NNW-SSE direction, sub-parallel to oblique to the strikes of the schistosity of metamorphic rocks distributed at the vicinity of the granitic rocks. YZ plan dips around 80 degree to SW or NE.

Similar to the distribution of the granitic rocks, the metamorphic rocks occur in a zone elongated in NE-SW direction. Quartz schist, muscovite-quartz schist, biotite schist, muscovite schist and slate are constituents of the metamorphic rocks.

The metamorphic rocks gradually change with, as a whole, decreasing metamorphic grade, that are, from east to west, quartz schist-muscovite quartz schist, biotite schist, muscovite schist and slate. The schistosity strikes NW-SE and dips at around 80 degree to SW of NE. Alternation of biotite schist and muscovite schist is partly observed, and they form small fold of few meters scale when blocks of muddy limestone of 1-5m across are included. The fold axes, same as Area A, trend in NW and plunge at around 45 degree.

Conglomerate and sandstone occur unconformably covering the metamorphic rocks. These, same as granitic rocks and metamorphic rocks, strike in NW-SE and dip at 30 to 40 degree. Both of these rock are considered to be the basement of the sedimentary rocks of post Triassic, distributed in western part of the area.

The mineralization in the area is azurite dissemination and malachite-azurite-calcopyrite-pyrite bearing quartz vein occurring in mylonite zone of granodiorite and schistose granite. The mineralization occurs in the fracture zones of country rock and locally dissemination of azurite occurs in the massive part of country rock. The occurrence of the latter suggests further extension of mineralization in the granodiorite body. The fracture zones trend in NW-SE to N-S.

4.10 Comprehensive Considerations

As the results of geological survey in the Attapeu Area, two sheets of 1:200,000 scale geological map and four sheets of 1:10,000 scale geological map were produced. Before the survey work of this project, only sparse information of the geology and mineral occurrences of the Attapeu area were available. Among these, two maps with relatively comprehensive information of the Attapeu Area are "Geological and Mineral Occurrence Map of LAO P.D.R., Scale 1:1,000,000" by DGM (1990) and "Geological Map of Cambodia, Laos and Vietnam (1991), Scale 1:1,000,000" by Geological Survey of Vietnam (1991). But these are small scale maps and, consequently, not having been enough for consideration of Time-Space development of geology/ore genesis and evaluation of potentiality of mineral resources. In addition to these, there had been many uncertainties concerning the occurrences of geological units and mineralization, and the ages of only a small number of stratigraphic sequences had been confirmed by the marine and non-marine index fossils. None of the ages of the igneous activities and ages of mineralization had been confirmed and the ages of these had been only predicted by relations between intrusive rocks and host rocks and similarity of their appearances.

Under the above mentioned situation, the geological survey of the Attapeu Area was conducted and the Geological and Mineral Occurrences Map at the scales of 1:200,000 and 1:10,000 were completed. All through the geological mapping work, various geological aspects of the area, such as detail geology, geological structure and mineral resources (distribution, characteristics, potential and ages of mineralization) of the Attapeu Area were clarified.

Based on the geological work of the Attapeu Area, comprehensive aspects of the geology and mineralization are summarized below.

4.10.1 Geology of the Attapeu Area

As shown in Figure 4.10.1, the geological aspects of the Attapeu area were summarized in the schematic columnar section produced based on the information obtained by the project, such as stratigraphic sequence, intrusive rocks, occurrences of mineralization, age determination.

The sedimentary sequences, igneous activities and tectonics of the Attapeu Area are summarized below.

i) Precambrian: igneous activities of mafic rocks (formation of oceanic crust?)

ii) Cambrian - Ordovician: sedimentation of oceanic to neritic sediments

iii) Ordovician - Silurian: sedimentation of oceanic to neritic sediments

iv) Silurian - Devonian: intrusion of I-type and A-type granite

v) Silurian - Devonian: metamorphic rocks of regional metamorphism (Caledonian)

vi) Devonian - Carboniferous: sedimentation of oceanic to neritic and non-marine sediments

vii) Devonian - Carboniferous: tectonic movement (Variscan)

viii) Carboniferous: intrusion of S-type granitic rocks

ix) Permian: intrusion of adakitic granitic rocks

x) Permian -Triassic: sedimentation of neritic to non-marine

xi) Triassic: volcanic activities of intermediate to acidic composition (intrusion and effusion of andesitic and rhyolitic volcanic rocks)

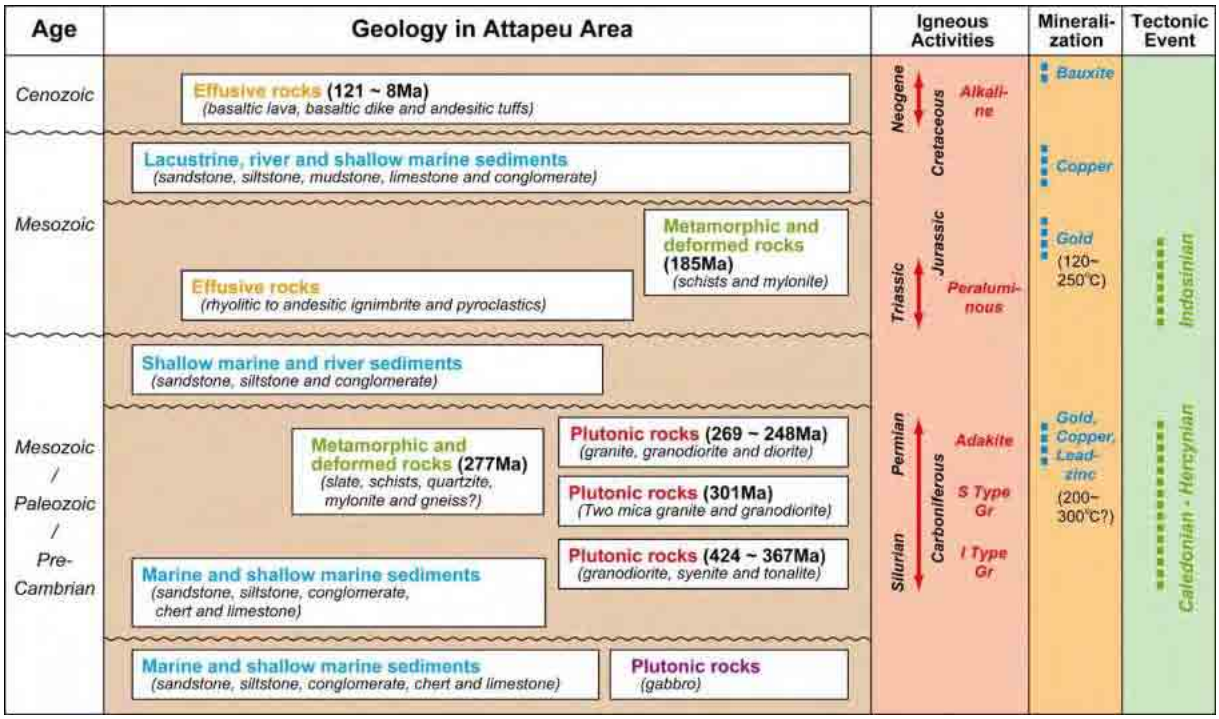

Figure 4.10.1 Schematic columnar section of Attapeu Area

xii) Permian-Triassic: tectonic movement (Indosinian)

xiii) Jurassic - Cretaceous: sedimentation of neritic to non-marine sediments

xiv) Cretaceous -Tertiary: volcanic activities of alkaline rocks (intrusion and effusion of lamprophyre)

xv) Cretaceous - Quaternary: volcanic activities of alkaline rocks (effusion of basaltic rocks)

As shown above, formation of sedimentary rocks started in Cambrian and continued to Cretaceous. The environments of sedimentations was oceanic to neritic at the beginning in Cambrian and after Permian it changed to neritic to non-marine and then after Cretaceous non-marine.

The igneous activities in the area started from formation of mafic rocks in Precambrian, and then followed by intrusion of granitic rock in Silurian to Permian. In Triassic, intrusion/effusion of intermediate to acidic rocks took place followed by intrusion and effusion of alkaline rocks in Cretaceous to Tertiary. Among these igneous activities, chemical nature of granitic magma related to the formation of granitic rocks change depending on the time of the activities as shown below.

i) Silurian: I-type granite (island arc)

ii) Devonian: I-type granite (island arc) to A-type granite (island arc to within plate)

iii) Carboniferous: S-type-adakitic granite (island arc)

iv) Permian: I-type-adakite granite (island arc)

The area encountered regional metamorphism in Silurian to Devonian. The mafic rocks of Precambrian and marine sediments of Cambrian to Silurian were metamorphosed to mainly pumpellyite-actonolite facies to green schist facies. After Devonian no clear evidence of formation of metamorphic minerals and metamorphic textures are observed. The metamorphic events in the area, therefore, are restricted in a period of after the formation of Silurian marine sediments and before formation of Devonian marine sediments.

The three periods of tectonic movements in the area, Silurian to Devonian, Devonian to Carboniferous and Permian to Triassic, were identified and each of which, respectively correspond to Caledonian, Variscan and Indosinian periods of tectonic movements. The characteristic features of each of the tectonic movement in the Attapeu Area are summarized below.

i) Silurian to Devonian (Caledonian): Occurrences of pumpellyite-actonolite facies to green schist facies metamorphic rocks.

ii) Devonian to Carboniferous (Variscan): Occurrences of pumpellyite-actonolite facies metamorphic rocks.

iii) Permian to Triassic (Indosinian): Occurrences of fractures zones characterized by mylonite and cataclasite.

4.10.2 Mineral Resources of Attapeu Area

As summarized below, variety of mineral resources including metallic, non-metallic and energy resources are found in the Attapeu area.

i) Metallic resources
- -gold (mesothermal, placer) : Vantat area.
- -copper (porphyry cupper, strata-bound sedimentary type): Attapeu East and eastern part of Xekong
- -bauxite and rare earth elements (residual deposits): Bolaven Plateau

ii) Non-metallic resources
- -industrial materials (ignimbrite): east of Attapeu.
- -feldspar (porphyritic granite): east of Attapeu.
- -Kaolinite (rhyolite): east of Attapeu.
- -benntonite (weathered soil): neighbors of Attapeu town
- -gem stones (ruby and sapphire): Nong Fa Lake area.

iii) Energy resources
- -coal (lignite): Dakchung area

The occurrences of these resources are shown in Figure 4.10.2.

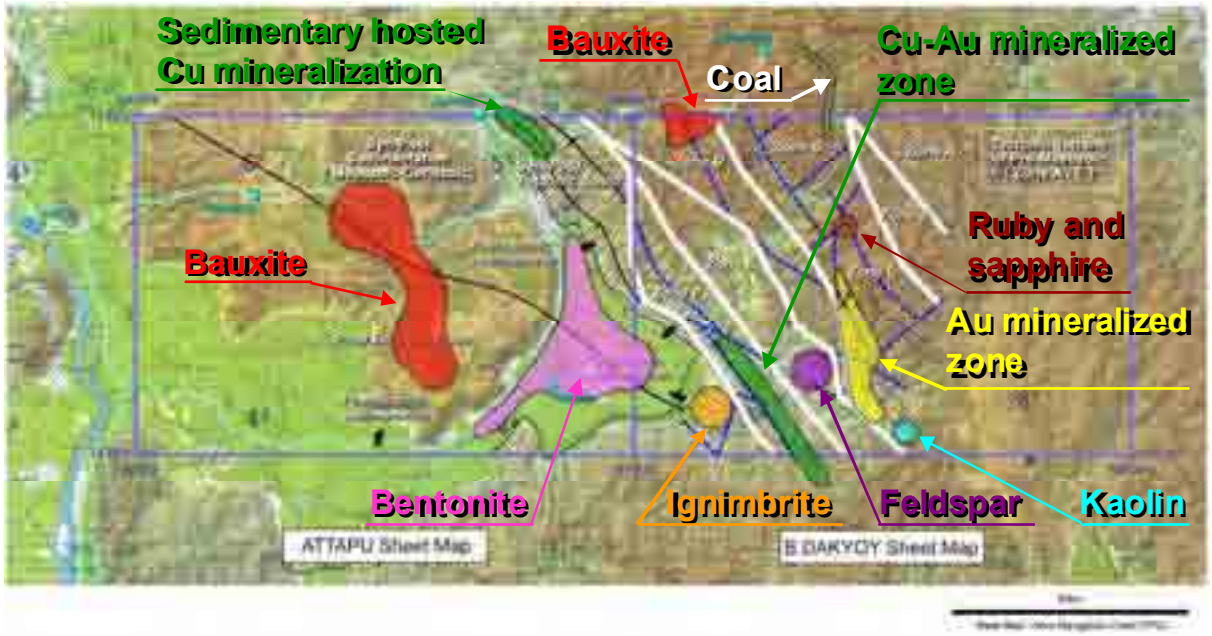

Figure 4.10.2 Occurrences of mineral resources in the Attapeu Area

Among the main mineral resources identified by the survey, these given below are considered to be economically important based on scale and extension.

a) Gold-Copper mineralization (Vantat area)

b) Copper-gold mineralization (Attapeu East Area)

c) Bauxite and rare earth elements (Bolaven Plateau)

Locations of the three main areas of mineralization are shown Figure 4.10.3.

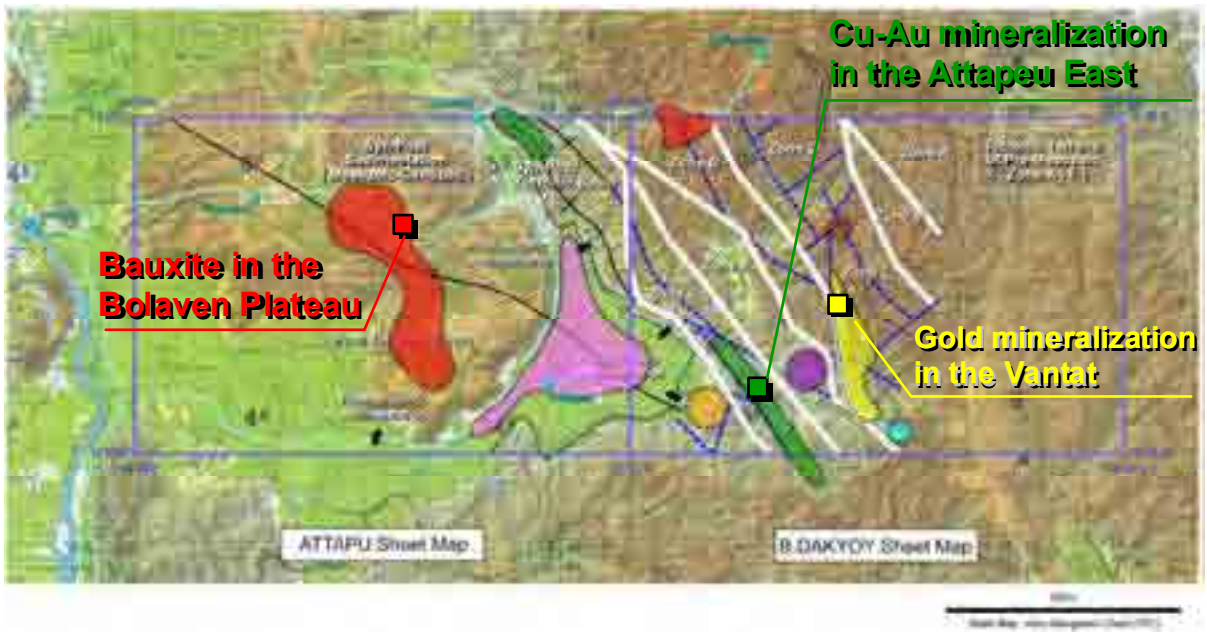

Figure 4.10.3 The main mineralization areas in the Attapeu Area

The characteristic features of these mineralization areas are given below.

1) Gold-Copper mineralization of the Vantat Area

The mineralization occurs in the protected area of the Laos national army and it was developed as a gold mine of the Laos National army. Production of gold was started in 2007. Geological and mineral resources map of the Vantat Area and its surrounding area, together with cross section of ore formation model are shown in Figure 4.10.4

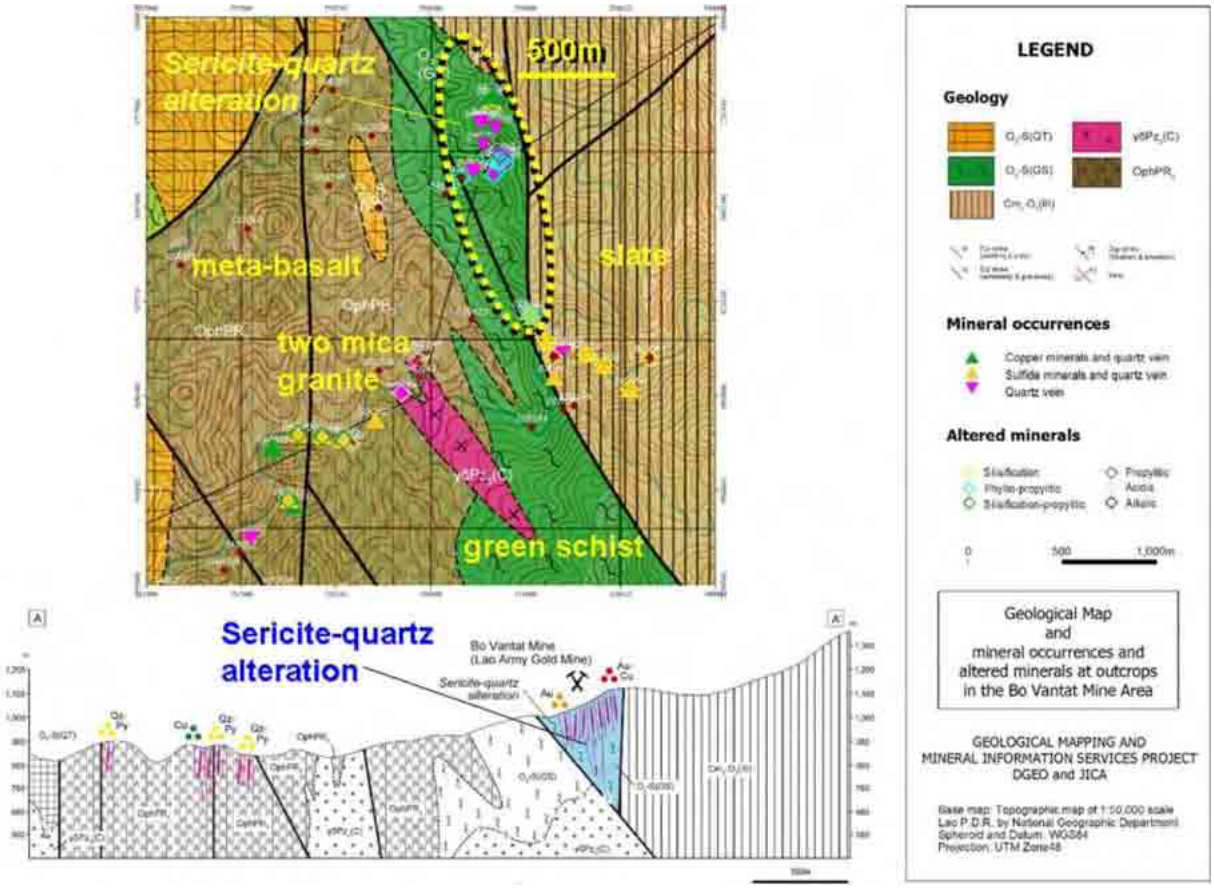

Figure 4.10.4 Geological and mineral resources map and cross section with ore formation model (Vantat Area)

The mineralization is characterized by dominant sericite-quartz alteration, nearly 200C degree of homogenization temperature of fluid inclusion of quartz veins, similar salinity of fluid inclusion to the veins of orogeny type gold mineralization and close association to fracture zones. These features of mineralization suggest the gold copper mineralization of the Vantat area to be low-sulfidation, mesothermal orogeny type. A summary of mineralization of Vandat area is given in Table 4.10.1.

Although a small scale mining operation is currently conducted in the Vandat area, since detail survey has not been done in the area, the scale of mineralization has not been known yet. Further, detail exploration work including surrounding area has not been done. For understanding the ore reserves of the mine and potentiality of the whole area, detail comprehensive survey including detail geological and mineralization surveys, geochemical survey (stream sediments, soil), geophysical survey (electric and magnetic) and drilling survey is necessary.

Table 4.10.1 Gold-Copper mineralization of Vantat Area

		Vantat Area
Mineral	Ore	native gold and pyrite
	Gangue	quartz
Occurrences		vein, argillation and fracture filling
Alteration		sericite, chlorite and rutile
Host rock		chlorite schist, basalt and pelitic schist
Related rock		two-mica granite?
Ore grade		237ppm Au, 22.2ppm Ag, 1.64% Cu for an altered rock with quartz veinlets
Mineralization type		orogenic mesothermal

2) Copper-gold Mineralization of Attapeu East Area

A new copper-gold mineralization was found during the project in the east of Attapeu along the Rout 18B, south of currently under contraction dam , Xe Kaman 1, and it was named as Attapeu East Area.

Geological and mineral resources map of the area together with cross section of ore formation model are shown in Figure 4.10.5.

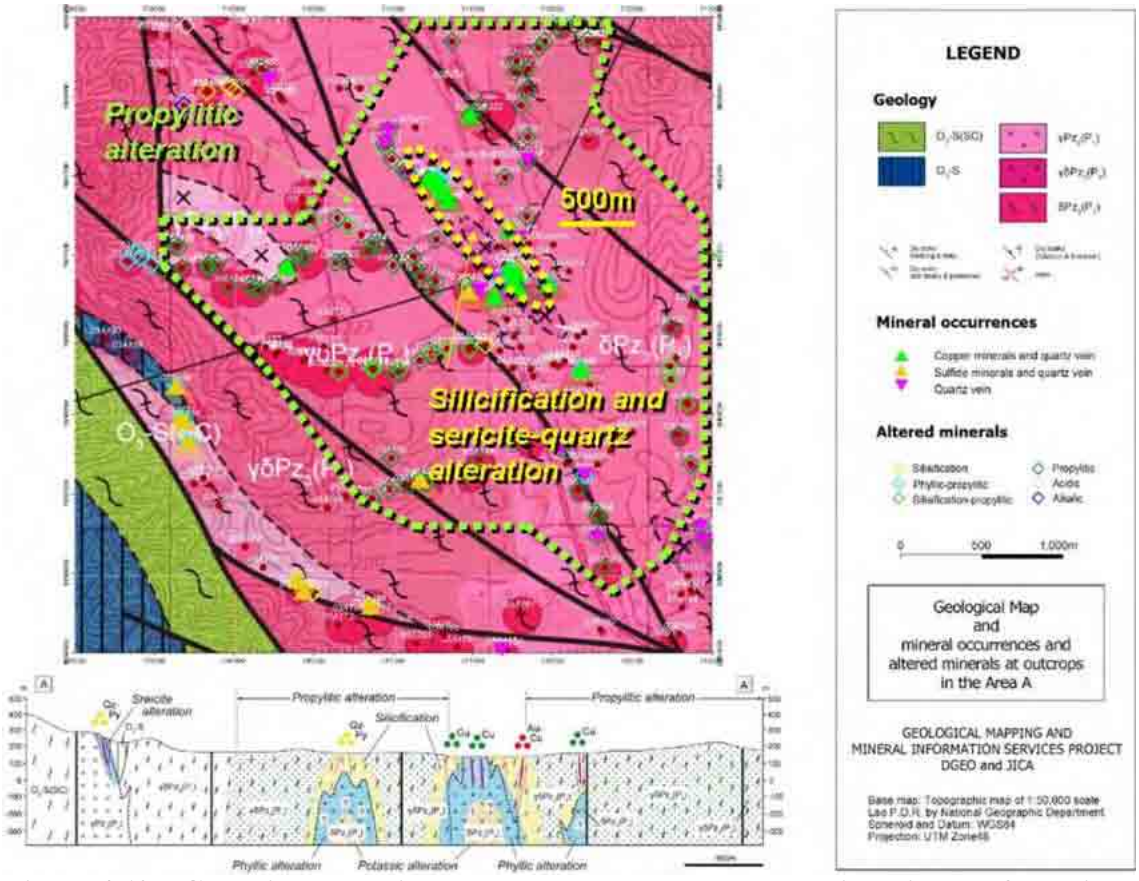

Figure 4.10.5 Geological and mineral resources map and cross section with ore formation model (Attapeu East Area)

Mineralization of the area is characterized by chlorite alteration of the host rock of the Cu-Au mineralization, sericite-quartz alteration at the center of mineralization, occurrences of stockwork quartz veins in the zone of sericite-quartz alteration. The features of mineralization and alteration of the area suggest that the mineralization of the Attapeu East Area is porphyry copper type.

A summary of mineralization of Attapeu East Area is given in Table 4.10.2

Table 4.10.2 Copper – Gold mineralization of Attapeu East Area

		Eastern part of Attapeu Area
Mineral	Ore	chalcopyrite, bornite, tenolite and pyrite
	Gangue	quartz
Occurrences		dissemination, vein and fracture filling
Alteration		sericite, chlorite, biotite and silicification
Host rock		granodiorite and tonalite
Related rock		mylonitic granodiorite and tonalite (adakite)
Ore grade		~ 6.55% Cu and ~ 6.9ppm Au for quartz veins, ~ 5.93% Cu for disseminated granodiorite
Mineralization type		porphyry Cu

The potentiality for economical mineral resources seems to be high in the area because of a wide distribution of Cu mineralization on the surface, high assay results of Cu and Au and possible type of mineralization being porphyry copper type. Further, Au and Cu anomalies extracted by stream sediments geochemical survey conducted during the project and findings of several bodies of granitic rocks possibly related to mineralization by analysis of satellite images suggest a fairly wide distribution of mineralized zone in the area.

Because of only surface information of mineralization is known, detail survey for confirming lateral and vertical extension of the mineralization is necessary in future for assessing potentiality of area. Detail geological and mineralization survey (route mapping and trenching), geochemical survey (stream sediments and grid survey of soil), geophysical survey (IP and magnetic survey) and drilling survey are recommended for understanding the scale of mineralization and assessing potentiality of the area.

3) Bauxite with high rare earth elements of Bolaven Plateau

Bauxite deposit with high rare earth elements occurs on the plateaus of the Bolaven Plateau and east of Xe Kong. Recently, exploration projects by foreign investments are actively conducted in these areas.

These are a residual type deposit formed near surface of alkali basalt and sandstone. The source of aluminum and rare earth elements are alkali basalt and the deposits were formed by enrichment of aluminum and rare earths elements through processes of weathering and erosion of alkali basalt.

Geological and mineral resources map of the area together with cross section of ore formation model and summary of mineralization are given in Figure 4.10.6 and Table 4.10.3, respectively.

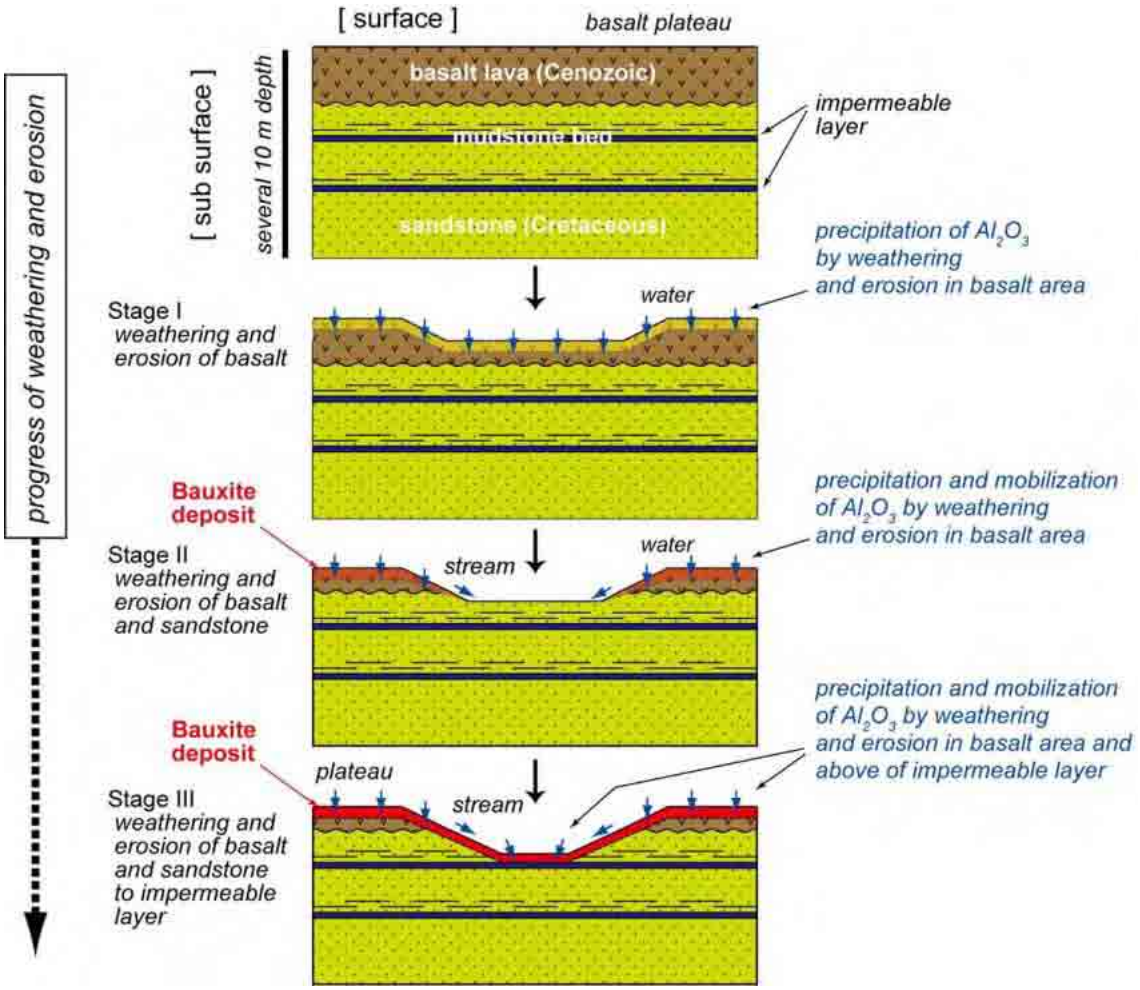

Figure 4.10.6 Cross section with ore formation model (Bolaven Area)

Table 4.10.3 Bauxite and REE mineralization of Bolaven Area

		Bolaven Area
Mineral	**Ore**	gibsite, goethite
	Gangue	opal
Occurrences		weathered soil near surface
Alteration		kaolin (weathering)
Host rock		basalt, sandstone
Related rock		alkali basalt
Ore grade		33.10% Al_2O_3, 37.90% Fe_2O_3, 939ppm REE for a bauxite.
Mineralization type		weathering residual near surface

The potentiality of the bauxite deposits with a wide spread distribution of lateritic soil in the area seems to be high. However, obtained grade of Al_2O_3 less than 40% in the area is rather low compared with general average grade of currently operating mine elsewhere, being more than Al_2O_3 40%. For assessing the potentiality of bauxite deposit of the area, it is necessary to extract sub-areas with more high concentration of Al_2O_3. For this purpose, it is necessary to conduct detail survey for understanding distribution of Al_2O_3 concentration in the area.

The total REE in the lateritic soil of the area is rather high, reaching more or less 1,000ppm. Particularly, total REE concentration of the clay layer between lateritic soil and host rock is high exceeding 2,500ppm. Among the REE, LREE, such as Ce, Nd, La, is higher, warranting further detail survey in the area. Detail geological survey (route survey and trenching) and drilling survey are recommended for understanding ore reserves of the area. For considering possible mine operation in the area, an efficient extracting methods of the REE must be considered in addition to confirmation of enough ore reserves.